Nisin-based coatings for the prevention of biofilm formation: Surface characterization and antimicrobial assessments

Mayssane Hage, Nour-Eddine Chihib, Marwan Abdallah, Simon Khelissa, Beatrice Crocco, Hikmat Akoum, Fouad Bentiss, Charafeddine Jama

Version of Record: https://www.sciencedirect.com/science/article/pii/S2468023021006362
Manuscript_fa7a6c9d5940f11caa9a6cebfba1017f

Nisin-based coatings for the prevention of biofilm formation: Surface characterization and antimicrobial assessments

Mayssane Hage [1,2], Nour-Eddine Chihib [1], Marwan Abdallah [1], Simon Khelissa [1], Beatrice Crocco [1], Hikmat Akoum [2], Fouad Bentiss [1,3], Charafeddine Jama [1,*]

[1] Univ. Lille, CNRS, INRAE, Centrale Lille, UMR 8207 - UMET - Unité Matériaux et Transformations, F-59000 Lille, France
[2] Laboratoire d'analyses chimiques et microbiologiques, Faculté de Santé Publique - Université Libanaise, Saida, Liban
[3] Laboratory of Catalysis and Corrosion of Materials, Faculty of Sciences, Chouaib Doukkali University, PO Box 20, M-24000 El Jadida, Morocco

* Corresponding author.
E-mail address: charafeddine.jama@centralelille.fr (C. JAMA).

ABSTRACT

Pathogenic bacterial biofilms invading surfaces in food and medical fields is a challenge to overcome. Despite all the strategies applied to fight against their formation, the biofilm microbiological risk remains as an important threat for populations. The prevention of biofilm formation might be an effective approach to confront this problem. In this study, stainless steel surfaces were functionalized by nisin, a natural antimicrobial peptide. Nisin was grafted onto the surface by either its carboxylic group or its amino group. The antimicrobial activity of the elaborated coatings was tested against *Listeria monocytogenes*. Indeed, the surfaces coated with nisin linked by its amino group showed an efficient antibacterial activity while the surface with nisin linked by its carboxylic group showed less antimicrobial effect. The surface properties analyses permitted to understand the chemical and topographical characteristics of treated surfaces including nisin conformation and quantification.

Keywords: Nisin*;* Stainless Steel; *Listeria monocytogenes*; Biofilms; Surface; Antimicrobial properties.

1. Introduction

Contamination of facilities with bacterial pathogenic biofilms in food and medical sectors is an ongoing problem and will be for many years if an efficient remedy is not found. Indeed, these pathogenic structures, formed on equipment, are involved in a variety of foodborne illness and nosocomial infections [1,2]. A study carried out by the Foodborne Disease Burden Epidemiology Reference Group (FERG), which was established by the World Health Organization (WHO) in 2007, estimated that 31 foodborne hazards caused 600 million foodborne illnesses and 420,000 deaths in 2010 [3]. On the other hand, health-care-associated infections, also defined as nosocomial infections are considered as the most common unfortunate events threatening patient safety worldwide [4-6].

Stainless steel (SS) is a widely employed material in agri-food and health domains for its appropriate properties. However, bacterial biofilms can develop and persist on SS-based equipment. The strategies of disinfections adapted by industrials and hospitals do not eliminate biofilms perfectly, especially the resistant ones. These plans aiming to control biofilm formation, affect negatively the environment, and have a consequent impact on the economy of these fields. Indeed, it's of great importance to find solutions to get rid of biofilm contamination.

The objective of this work is to design an effective tool to fight against biofilm formation. The elaboration of surfaces with antimicrobial bacteriocin-based coatings seems to be a powerful remedy in killing pathogenic bacteria. Moreover, the use of antimicrobial peptides (AMPs) adsorbed onto surfaces is one of the possible innovative and proactive approaches to prevent contaminations and infections [7]. Nisin is a member of these antimicrobial peptides which can be grafted on materials. It is a positively charged polypeptide with a 3500 Da molar mass presenting 34 amino acid allocated in hydrophilic residues at the COOH-terminus and hydrophobic residues at the NH_2-terminus (Fig. 1). It is known as a safe food additive and has been accepted and applied in food preservation in over 50 countries for a

period of almost 40 years [11]. It is produced by *Lactococcus lactis* subsp. *lactis* and have an interesting inhibitory effect on a large number of Gram-positive bacteria, including *Listeria monocytogenes* and *Staphylococcus aureus* [12]. *L. monocytogenes* is a Gram positive bacteria involved in Listeriosis a foodborne illness. Its fatality rate is around 30%, possibly higher for pregnant women and people with weakened immune system [13].

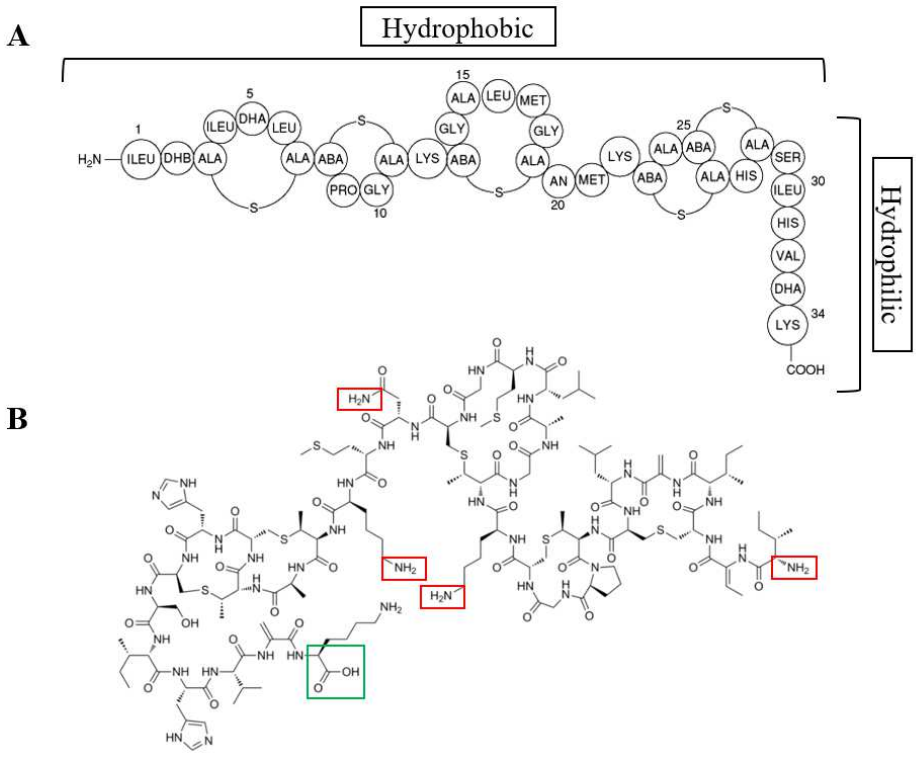

Fig. 1. (A) Primary structure of nisin A presenting the 34 amino acids distribution in the hydrophobic and hydrophilic parts (adapted from [13]) (B) Chemical structure of nisin showing NH_2-terminus and COOH-terminus (adapted from [14]).

In this work, two approaches of nisin conformation linkage were applied in the coating elaboration. The first approach was the linkage of nisin by its amino group while its only carboxylic group was free. The second one was to link the nisin by its only carboxylic group while its amino groups were free. In the process, firstly, dopamine was polymerized on SS in order to acquire amino groups on the surface. After that, according to the first approach of nisin linkage, glutaraldehyde was fixed between polydopamine and nisin, which was added finally,

resulting in a model surface called stainless steel/polydopamine/glutaraldehyde/nisin (SDGN). Moreover, according to the same approach, succinic acid was linked to polydopamine, and nisin was grafted in the end, resulting in a model surface called stainless steel/polydopamine/succinic acid/nisin (SDAN). In the second linkage approach, nisin was directly attached by its carboxylic group to polydopamine without a linking agent resulting in a model surface called Stainless steel/polydopamine/nisin (SDN). Fig. 2 explains the linkage approaches. In a recent study, a glass surface was modified via electron-transfer and chemical reactions employing dopamine to attach nisin directly. The results of XPS and FTIR showed that nisin was successfully grafted. Moreover, the modified surfaces inhibited the adhesion of both algae *Phaeodactylum tricornutum* and bacteria *Bacillus* spp. [14]. Otherwise, according to several studies, the most common cross-linker used is glutaraldehyde. However, unfortunately it is toxic [15]. In the search for a potential harmless analogue, succinic acid which is a dicarboxylic acid, was selected. Succinate is a food additive used as an acidulant/pH modifier, as a flavoring agent in the food markets. It is also used in the markets of production of health-related agents, including pharmaceuticals, antibiotics, amino acids, and vitamins [16]. Indeed, succinic acid is generally recognized as safe by the U.S. Food and Drug Administration [17].

In order to characterize these coatings before and after the nisin immobilization, in term of antimicrobial and chemical properties, several analyses were carried out. The antimicrobial efficiency of the treated surfaces was carried out towards *L. monocytogenes.* Firstly, the adhesive power test of treated surfaces was performed to analyze the comparability of bacterial adhesion rates on each treated surface. Secondly, an indirect antibacterial evaluation of the treated surfaces was carried out via a challenge test. In addition, a direct antibacterial evaluation was carried out via the LIVE/DEAD Kit, qualitatively testing the surfaces on a bacterial lawn, and Scanning Electron Microscopy (SEM) analysis of the bacterial state. The chemical analysis and the molecules conformation and presence was demonstrated via water contact angle (WCA)

measurements, Fourier transform infrared analyses (FTIR), surface roughness and thickness, SEM analyses, Time-of-flight secondary ion mass spectrometry (ToF-SIMS) and X-ray photoelectron spectroscopy (XPS).

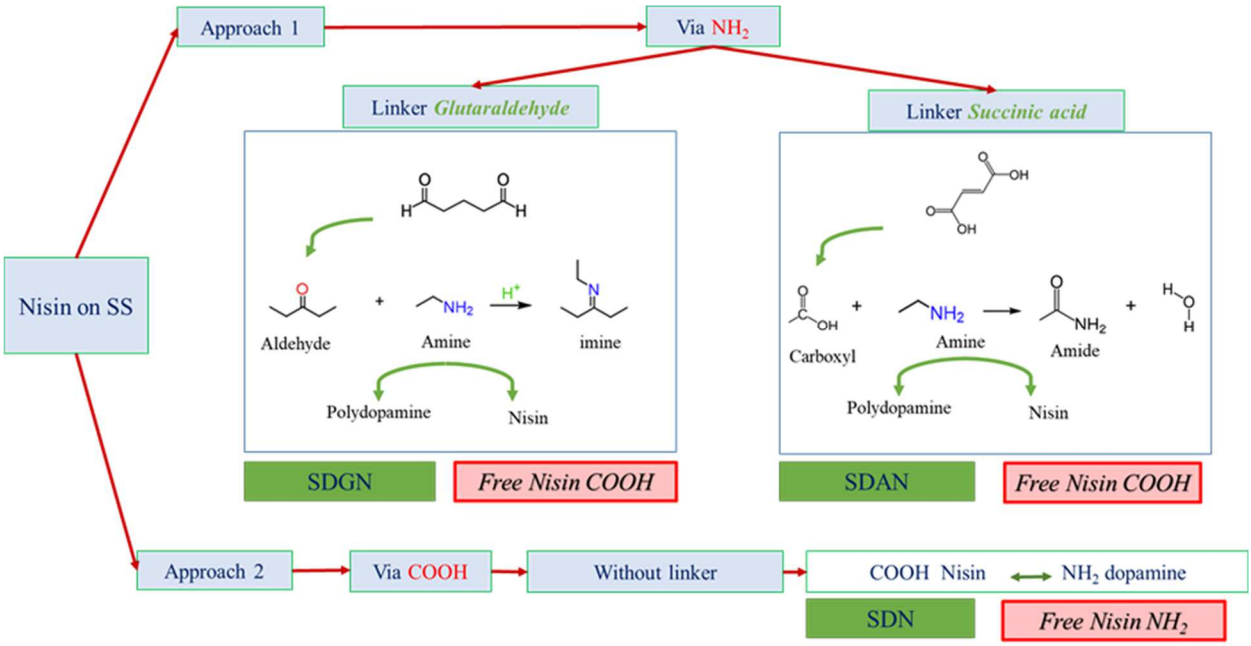

Fig. 2. Schematic representation of nisin grafting approaches.

2. Material and methods

2.1. Standardized SS slides preparation

The SS circular slides, purchased from Acciai Speciali Terni (Terni, Italy) and polished by Equinox (Willems, France), are 40 mm of diameter and 1 mm of thickness. After removing the SS protection film, the slides were soaked for 10 min in absolute ethanol (Brabant, France), then rubbed with a paper towel dipped with ethanol in order to remove the sticky residues of the protection films. They were then air-dried and autoclaved at 120°C for 20 min for sterilization. SS slides were then collected in sterile Petri dishes.

2.2. Bacterial strain, culture conditions and suspension preparation

Listeria monocytogenes ATCC 35152 (LM/NCTC, United Kingdom) is the bacterial strain selected for this research. The cryogenic vials containing this strain with Tryptic soy broth (TSB; Biokar Diagnostics, France) and 40% (v/v) of glycerol were stored at – 20°C. For pre-culture preparation, 100 µl of the frozen tubes was inoculated into 5 ml of TSB and then incubated at 37°C. After 24 h of incubation, in order to prepare the culture of *L. monocytogenes,* 100 µl of this pre-culture that contains 10^4 CFU ml^{-1} was inoculated into 50 ml of TSB culture medium in 500 ml sterile Erlenmeyer. The culture was incubated at 37 °C under stirring condition at 160 rpm, and bacterial cells were collected in the late exponential condition after 15 h. *L. monocytogenes* cells were collected by culture centrifugation (5000 g, 10 min, 20 °C) and washed twice with 20 ml of sterile physiological saline solution (Saline; 0.85%) to purify and eliminate the solution from TSB and bacterial debris. Finally, cells were re-suspended in 20 ml of saline. The *L. monocytogenes* suspension was prepared to a concentration of (1×10^8 CFU ml^{-1}) via spectrometric reading (Jenway 6320D spectrophotometer). It was then sonicated at 37 kHz for 5 min at 20 °C (Elma S40 Elmasonic, Germany) for cell dispersion. This bacterial suspension was then diluted 10 fold to a specific concentration depending on each bacterial test.

2.3. Coatings elaboration protocols

2.3.1. Stainless steel/polydopamine (SD) coatings

Dopamine hydrochloride H8502-25G (Sigma-Aldrich, France) was dissolved in Tris-Base buffer solution (10 mM) in order to obtain a solution of 2 mg ml^{-1} and pH was rectified to 8.5 using sodium hydroxide solution (2 M). Then 20 ml of solution were spilled in a Petri dish of 8.5 cm of diameter containing two standardized SS slides. The Petri dish was incubated at 20 °C for 24 h under stirring condition at 160 rpm after its wrapping in parafilm. This continuous agitation allows homogeneous polymerization of dopamine hypochloride to

polydopamine and prevents the deposition of undesirable microparticle on the samples. After incubation, the slides were gently rinsed four times with 20 ml of autoclaved ultrapure water (Milli-Q IX Pure Water System). These coated surfaces are called SD. All the treated surfaces hereafter were incubated and rinsed in the same conditions as SD.

2.3.2. Stainless steel/polydopamine/nisin (SDN) coatings

The antimicrobial peptide nisin (Danisco Beaminster Dorset, United Kingdom), being insoluble in water was dissolved in hydrochloric acid solution 0.01 M. The dissolution was carried out gently avoiding foam formation. N-(3-Dimethylaminopropyl)-N'-ethylcarbodiimide hydrochloride (EDC) and N-Hydroxysuccinimide (NHS) 98% (Both purchased from Sigma-Aldrich, France), were dissolved in phosphate buffer pH = 6.2 and added to the prepared nisin solution (1 mg ml^{-1}). The final concentration of EDC and NHS was 0.02 M and 0.01 M, respectively. To immobilize nisin, 20 ml of the solution were directly poured into a Petri dish containing two SD samples. The system was incubated then rinsed in the standardized condition. These coated surfaces are called SDN.

2.3.3. *Stainless steel/polydopamine/glutaraldehyde/nisin (SDGN) coatings*

Glutaraldehyde (Sigma-Aldrich, France), employed as a spacer arm, was diluted in sterile ultrapure water to 3%. 20 ml of this solution was poured into a Petri dish containing two samples of SD. The system was incubated then rinsed in the standardized condition. These coated surfaces are called SDG. Nisin was dissolved gently in hydrochloric acid solution 0.01 M (Using the rate Nisin : HCl = 10mg:1ml). Then, the solution was diluted in sterile ultrapure water in order to obtain a concentration of 1 mg ml^{-1}. The pH is then neutralized to 7 by addition of sodium hydroxide solution (2 M). Then 20 ml of the solution were spilled into a Petri dish containing two rinsed SDG. The system was incubated then rinsed in the standardized condition. These coated surfaces are called SDGN.

*2.3.4. Stainless steel/polydopamine/*succinic acid */nisin (SDAN) coatings*

A solution containing 3% of succinic acid (Janssen-Beerse, Belgium), 0.02 M EDC and 0.01 M NHS was prepared in phosphate buffer (pH = 6.2, 10 mM). The pH of the solution was adjusted to 4.3 by adding 2 M of sodium hydroxide solution. Then 20 ml of this solution were poured into a Petri dish containing two SD samples. The system is incubated then rinsed in the standardized condition. These coated surfaces are called SDA. For the elaboration of nisin-coated SDA, the same steps of SDA preparation were followed, changing the incubation time of the solution before adding nisin. Indeed, 19.5 ml of the solution were poured in a Petri dish that was closed with parafilm and incubated at 20°C under stirring at 160 rpm for 3 h. After this time, 0.5 ml of the dissolved nisin (1 mg ml^{-1}) in hydrochloric acid solution of 0.01 M were added into the Petri dish and incubated again on the stirring plate for 21 h at 20 °C. After this time, the standardized rinsing protocol was followed. These coated surfaces are called SDAN.

2.4. Bacterial adhesion tests in NEC biofilm system

Visualization of adhered bacteria on coated surfaces was carried out with epifluorescence microscopy 100 × magnification (Nikon Optiphot-2 EFD3). Bacterial adhesion test allows to quantify the number of cells adhered on a surface that has been put in contact with a bacterial suspension. This analyze aimed to prove a comparability of the number of adhered bacteria between all the surfaces. The bacterial adhesion test was carried out on the prepared coated surfaces and non-coated SS by exposing them to a *L. monocytogenes* suspension in *NEC biofilm system* [18]. Bare SS was taken as control. Briefly, 5 ml of 10^7 CFU ml^{-1} *L. monocytogenes* suspension were statically incubated on each sample at 20°C for 1 h to allow bacterial adhesion. The solution was then removed, and coupons were rinsed with 20 ml of sterile physiological water to eliminate all loosely attached cells. The adhered cells were then stained with 2 ml of acridine orange (AO) 0.01% (w/v) for 10 min in darkness. After this time,

the intercalating agent was withdrawn, and the coupons were rinsed twice with 2 ml of physiological water to clear out excess of AO. The samples were then dried and observed under the microscope. A total of 25 fields per coupon were captured with a digital camera and stained cells were enumerated. Mean value of adhered bacteria per microscopic field and its relative standard deviation were presented. Three repetitions were carried out for each coating type.

2.5.Antibacterial challenge test

After the adhesion rate test, the challenge test was carried out by treated surfaces, towards *L. monocytogenes* to assess the antimicrobial activity of these surfaces, specifically of the ones grafted with nisin. Uncoated SS was taken as a control. The protocol for the challenge test was carried out according to the procedure proposed in the norm ISO 22196 [19]. The concentration of *L. monocytogenes* solution tested was 10^5 CFU ml^{-1} prepared in diluted TSB to 1/100 volume. Each coating was collected in a sterile pot and 1 ml of the test inoculum was deposited on the entire surface for 3, 5 and 24 h under sterile condition, at 20 °C. After incubation, the 1 ml of deposited bacterial solution and the sample were recovered and placed upside down in a sterile container containing 9 ml of sterile tryptone salt (Biokar, France) solution (9.5 g l^{-1}). In order to unhook the cells, the container was vortexed for 15 seconds, sonicated in an ultrasonic bath for 5 min at 37 kHz at 20°C (Elmasonic S60H, Elma, Germany) and again vortexed for 15 seconds. Then 10-fold dilution was performed for each condition. The bacteria were enumerated by mass enumeration technique in Tryptone Soy Agar (TSA; Biokar Diagnostics, France) after incubation at 37°C for 24 h. The mortality rate of bacteria on a coated SS was assessed by comparing the relative colony-forming unit (CFU) to the one associated to the uncoated SS. Logarithmic reduction of CFU was then calculated. Three repetitions were carried out for each coating type.

2.6. Assessment of the bacterial viability with the Live/Dead backlight viability kit

The viability test of bacteria exposed to treated surfaces was carried out. Bare SS was taken as a control. Briefly, after 3 and 5 h of exposure to coupon's surface, the 1 ml of 10^5 CFU ml^{-1} of bacterial solution on each coupon is mixed to 4 ml of sterile tryptone salt solution. For each coupon condition, bacterial solutions were stained with LIVE/DEAD BacLight Bacterial Viability kit (Invitrogen Molecular Probes, USA), according to the manufacturer instruction for 15 min in the dark. After this time, 1 ml of the solution is vacuum filtered through a 0.2 µm pore-size polycarbonate membrane filters (Millipore, France). Stained cells were washed once with 1 mL of saline solution (0.85% of NaCl) and filters were placed on microscopic slides for the epifluorescence microscopic enumeration. The viable and dead cells were counted in 25 microscopic fields. Results are expressed as mean (± Standard deviation) of three repetitions for each coating type.

2.7. Qualitative antibacterial test of treated surfaces

The qualitative testing was carried out on all the treated surfaces to assess the antibacterial activity of efficient nisin coated surfaces and prove the nisin linkage to the films without its diffusion. Mueller Hinton agar medium (Biokar Diagnostics, France) was seeded with *L. monocytogenes*. The face-up of the treated surfaces were placed on the agar surface. The plate was incubated at 20 °C for 3 h for nisin activity. The films were then removed and the plate was incubated at 37 °C for 24 h. Nisin activity was assessed as an inhibition of *L. monocytogenes* growth on the zone where the film was placed without its diffusion. The nisin diffusion was underlined as control, via pure nisin soaked cellulose disc employed on the media.

2.8. Water contact angle measurements

Water contact angle (WCA) measurements were obtained by on a DSA100 drop shape analyser (Krüss, Germany). Droplet of 2 µl deionized water were deposited onto the surface of

samples at room temperature. Measurements were taken on five different areas of each coupon. Contact angle was calculated with Advance software. Data are representative of three different measurements on five droplets deposed randomly on the coating surfaces.

2.9. Surface roughness and thickness analyses

The surface roughness of the coatings was determined using a surface profiler Alpha-step IQ (Kla Tencor, Milpitas, California). Samples were scanned over a length of 1 mm with a scan speed of 20 µm s^{-1} and sampling rate of 50 Hz. Each sample was scanned in three locations. The resolution was 400 nm. SS was always taken as control. The average roughness (R_a) and the root-mean-squared roughness (R_q) were presented and calculated using the following equations:

$$R_a = \frac{1}{n}\sum_{i=1}^{n}|Y_i| \quad (1)$$

$$R_q = \sqrt{\frac{1}{n}\sum_{i=1}^{n} Y_i^2} \quad (2)$$

The thickness of the treated surfaces was also measured. A tape was stuck on a part of the SS slide before its treatment. After coatings elaboration on those samples, the tape was removed and the thickness was measured on 5 different zones. The average values for coatings thickness were then calculated with its standard deviation.

2.10. Scanning Electron Microscopy analysis

Scanning Electron Microscopy was carried out to visualize the morphology of bare SS, coated surfaces, and to observe the state of bacteria in contact with coatings. SEM micrographs were taken at 20,000× magnifications. Standard procedures for fixing and embedding sensitive biological samples were carried out on coatings with adhered bacteria. SEM analyses were done using a Hitachi S-4700 SEM equipped with a field emission gun (FEG). Beforehand the observations, samples were sputter coated with carbon to become conductive with BAL-TEC SCD 005 Sputter Coater.

2.11. Ion polishing of coatings

Prior to SEM imaging, sample cross sections were first polished using SiC polishing sheets up to a grade 1200 and then using a Fischione Instruments 1061 SEM Mill ionic polishing system at 4 kV for 2 h to obtain a smooth surface. Prepared samples were carbon coated with a Bal-Tec SCD005 sputter coater and SEM images were taken using a JEOL JSM 7800F LV scanning electron microscope at 5 kV.

2.12. Fourier Transform Infrared analysis

The FTIR spectra of treated surfaces were recorded by a Fourier Transform Infrared (FTIR) spectrometry (Nicolet iS50 FT-IR spectrometer - Thermo Scientific Waltham, USA) at room temperature. 64 spectral scans were recorded, which was sufficient to achieve good resolution. All the spectra were analyzed using OMNIC software.

2.13. ToF-SIMS analysis

ToF-SIMS is a surface analytical technique. In this method, a pulsed beam of primary ions already passed over the surface of the sample, produces secondary ions in a sputtering process. Analyzing the secondary ions provides information about the molecular and elemental species present on the surface. ToF-SIMS measures were performed on a ToF.SIMS 5 instrument by ION-ToF GmbH (Germany). It was equipped with a Bi liquid metal ion gun (LMIG). The measurements were carried out with pulsed primary Bi^{3+} ions. (25 keV and 0.4 pA). A low-energy (20 eV) electron flood source was employed for charge compensation. For each coating, positive and negative mass spectra were picked from a surface of 500 x 500 mm corresponding to 30 scans. Data were analyzed using SurfaceLab 6.2 software.

2.14. XPS analysis

XPS measures were performed using XPS KRATOS, analytical AXIS UltraDLD spectrometer Thermo Scientific KAlpha XPS system (UK). The monochromatized Aluminium-Kα X-ray source (hv = 1486.6 eV) was carried out via an electromagnetic lens mode and in a constant analyzer energy mode (CAE = 150 eV for survey spectra and CAE = 30 eV for high resolution spectra). The binding energy scale was initially calibrated using the Ag $3d_{5/2}$ (368.2 eV), Cu $2p_{3/2}$ (932.7 eV) and Au $4f_{7/2}$ (84 eV) peak positions. In addition, the C 1s hydrocarbon (285.0 eV) binding energy (BE) was used as internal reference for calibration. Simulation and quantification of the experimental peaks were performed using the CasaXPS software. Moreover, quantification took into account a nonlinear Shirley background subtraction [20].

2.15. Statistical analysis

All quantitative measurements were reproduced in triplicate. Statistical analysis was carried out with IBM SPSS 19 statistics software using one-way ANOVA. Results were considered significantly different when $p < 0.05$.

3. Results

3.1. Antibacterial effect of nisin coated SS

Bacterial adhesion test was carried out to ensure that coatings had comparable adhesion rates before performing antibacterial activity tests. Bacterial adhesion test on bare SS showed an average of 26 ± 5 adhered *L. monocytogenes* per microscopic field. The average of adhered cells per microscopic field obtained for each coating type was comparable for all coating types (Fig. 3). Indeed, the adhesion rate was 18 ± 2, 20 ± 3, 20 ± 3, 27.5 ± 4, 23 ± 2 and 25 ± 3.5 for SD, SDN, SDG, SDGN, SDA and SDAN, respectively. Fig. 4 shows one microscopic field representing the tendency of adhered bacteria on each sample.

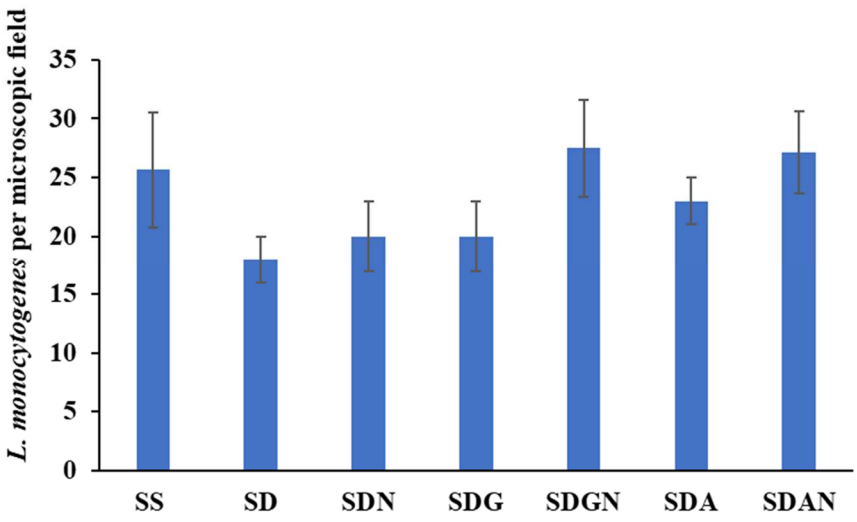

Fig. 3. Assessment of *Listeria monocytogenes* adhesion on SS, SD SDN SDG SDGN SDA and SDAN.

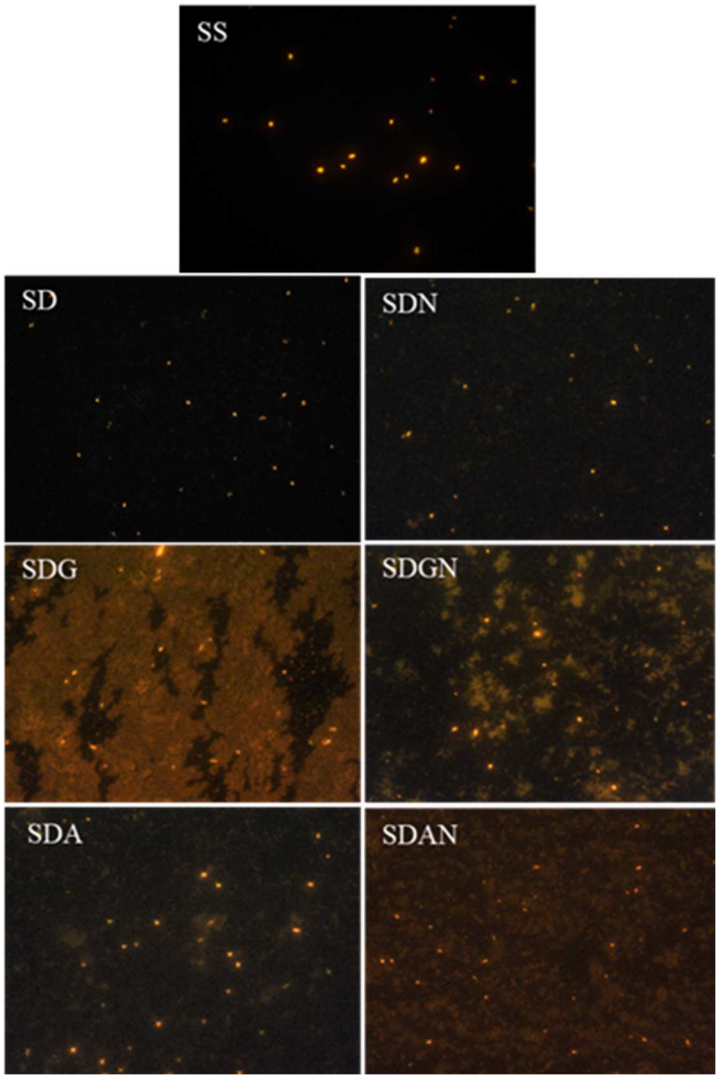

Fig. 4. *Listeria monocytogenes* adherent cells on different coated SS. Acridine orange staining and epifluorescence microscopy were used to assess *L. monocytogenes* adhesion capabilities.

In order to characterize the antibacterial activity of coated surfaces, a challenge test adapted from the antibacterial ISO 22196 test against Gram positive bacteria, was carried out . After 3 h of *L. monocytogenes* contact with SS, SD, SDG and SDA, the bacterial load was log 5.26 ± 0.04, log 5.18 ± 0.02, log 5.16 ± 0.04 and log 5.15 ± 0.03 CFU cm^{-2} respectively. After 5 h, SS, SD, SDG and SDA registered a similar logarithm tendency of 3 h. Indeed, it was 5.36 ± 0.03, 5.21 ± 0.06, 5.22 ± 0.02 and 5.17 ± 0.04 CFU cm^{-2} respectively. Nisin coated SDN registered after 3 and 5 h a bacterial logarithm of 5.17 ± 0.05 and 5.17 ± 0.09 respectively.

Otherwise, for SDGN and SDAN, the bacterial logarithm obtained decreased of almost 2 and 1.5 CFU cm^{-2} respectively. Indeed, SDGN registered after 3 and 5 h a bacterial logarithm of 2.20 ± 0.17 and 2.55 ± 0.12 CFU cm^{-2} respectively, and SDAN registered after 3 and 5 h a bacterial logarithm of 3.47 ± 0.05 and 3.55 ± 0.04 respectively CFU cm^{-2}. After 24 h of bacterial contact, the bacterial logarithm increased for all coated surfaces. In fact, SS, SD, SDN, SDG, SDGN, SDA and SDAN registered respectively logarithmic values of 7.29 ± 0.10, 7.17 ± 0.07, 7.08 ± 0.05, 7.19 ± 0.03, 7.08 ± 0.08 and 7.21 ± 0.04 CFU cm^{-2} (Fig. 5).

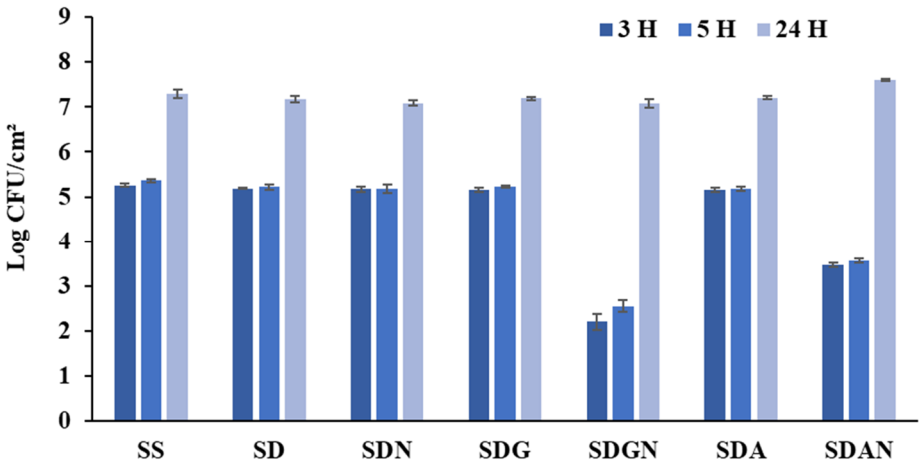

Fig. 5. Antimicrobial assessment of the different treated SS surfaces on *Listeria monocytogenes*.

Otherwise, bacterial solution incubated for 3, 5 and 24 h upon control and nisin-coated substrates, was stained by LIVE/DEAD Kit and observed using the epifluorescence microscopy. The enumeration of viable cells, underlined that *L. monocytogenes* on SS, SD, SDG and SDA registered predominantly viable cells after 3 and 5 h. Moreover, the bacterial viability after 24 h had the same tendency for SS and all coated surfaces with or without the antimicrobial nisin. Otherwise, bacterial viability decreased of 60 % and 50% after 3 and 5 h of contact with SDGN and SDAN respectively while SDN did not decrease the bacterial viability (Fig. 6).

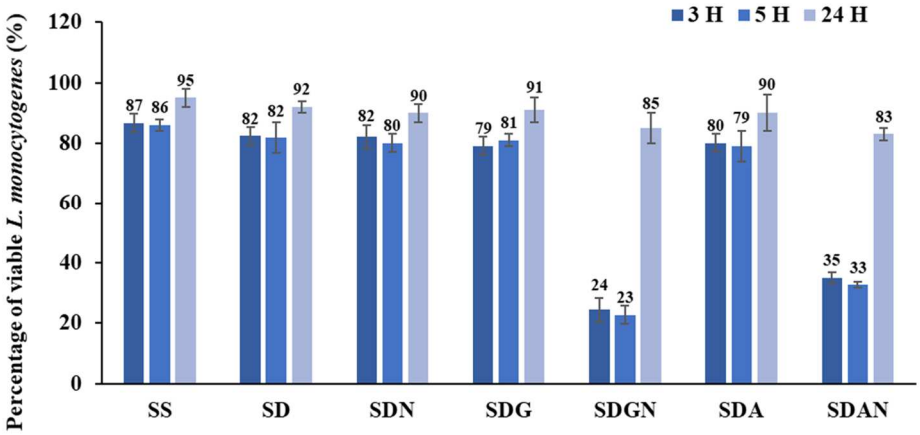

Fig. 6. Viability percentage of *L. monocytogenes* with LIVE/DEAD kit after 3, 5 and 24 h of contact with SS and coated SS surfaces (± SD).

SEM analyses were carried out to observe the bacterial state around effective antimicrobial coatings, SDGN and SDAN. SS was taken as a control. *L. monocytogenes* state was intact and the cell wall presented no degradation after 3 and 5 h of contact with SS (Fig. 7A and 7D). Otherwise, SEM micrographs in Fig. 7B, 7C, 7E, and 7F showed the damaged cell wall of *L. monocytogenes* on SDGN and SDAN after 3 and 5 h of contact. Nisin granulations were clearly detected near the bacteria (Fig. 7).

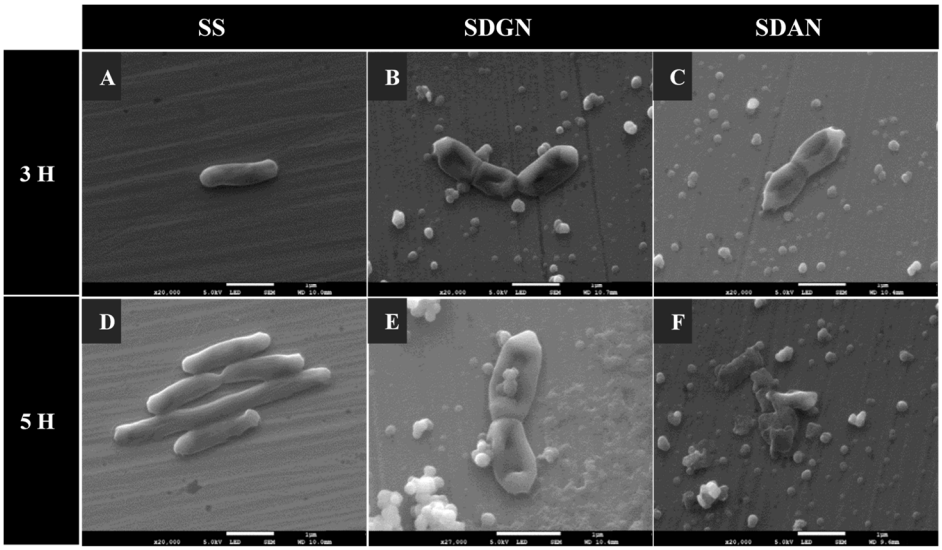

Fig. 7. Scanning Electron Microscopy micrographs showing the state of *Listeria monocytogenes* adhered to non-coated SS surface (A-D) and to coated SS surfaces (B-C-E-F) after 3 and 5 hours of contact with the surfaces.

The antibacterial qualitative test showed a significant antibacterial activity linked to SDGN and SDAN while SDN did not show an inhibition zone. SS, SD, SDG and SDA, taken as control did not show any antimicrobial activity. Cellulose disc soaked in pure nisin showed a diffusion circle while no diffusion was observed for SDGN and SDAN as shown in Fig. 8.

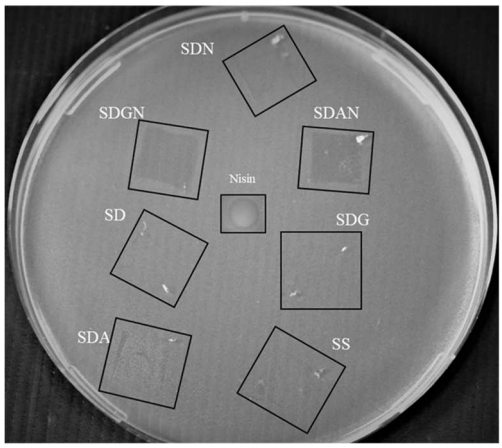

Fig. 8. Antibacterial assessment toward *Listeria monocytogenes* of different coated SS surfaces and nisin (1 mg ml^{-1}). The experiment was performed on Mueller Hinton agar medium was seeded with *L. monocytogenes*.

3.2.Surface characterization of SS coated films

In order to understand the properties of treated surfaces, the presence of molecular compounds and their relative quantities and nisin conformation on coatings, different tests for analyzing the chemical properties of the treated surfaces were carried out.

WCA was measured on the different treated surfaces to make sure that nisin is fixed onto SDGN, SDAN and SDN samples. WCA of bare SS was 61 ± 2°. Treated surfaces SD, SDG and SDA generated a decrease in the WCA, to 54 ± 1°, 42 ± 3° and 42 ± 2° respectively. These coatings provided the steel surface a more hydrophilic character. However, after nisin addition to pretreated surfaces (SD, SDG and SDA), SDN, SDGN and SDAN were characterized by higher WCA measurements that went from 81 ± 3°, 83 ± 3° and 73 ± 2° respectively (Table 1).

Table 1

WCA measurements on bare and different treated surfaces.

Surface	WCA (°)	Standard deviation (°)
SS	61	± 2
SD	54	± 1
SDG	42	± 3
SDA	42	± 2
SDN	81	± 3
SDGN	83	± 3
SDAN	73	± 2

The surface roughness of coatings was analyzed by Alpha-Step IQ, stylus-based surface profiler. Bare SS was characterized by a roughness R_a equal to 2.8 ± 0.1 nm and R_q equal to 3.9 ± 0.4 nm. After polydopamine immobilization on the SS surface (SD) the roughness values decreased to R_a equal to 1.9 ± 0.3 nm and R_q equal to 2.5 ± 0.4 nm. For SDN, after nisin grafting on SD, roughness increased significantly to 4.8 ± 0.8 and 6 ± 0.3 nm for R_a and R_q respectively.

SDG showed a similar roughness to bare SS and SDA presented a higher roughness values R_a equal to 3.4 ± 0.5 nm and R_q equal to 4.4 ± 0.5 nm. Otherwise, the nisin fixation on SDG and SDA, barely increased the roughness of almost 0.5 nm for SDGN and 1 nm for SDAN. Indeed, SDGN registered 3.08 ± 0.2 nm for R_a and 4.01 ± 0.2 nm for R_q and SDAN registered 4 ± 0.43 nm for Ra and 5.39 ± 0.36 nm for R_q (Fig. 9).

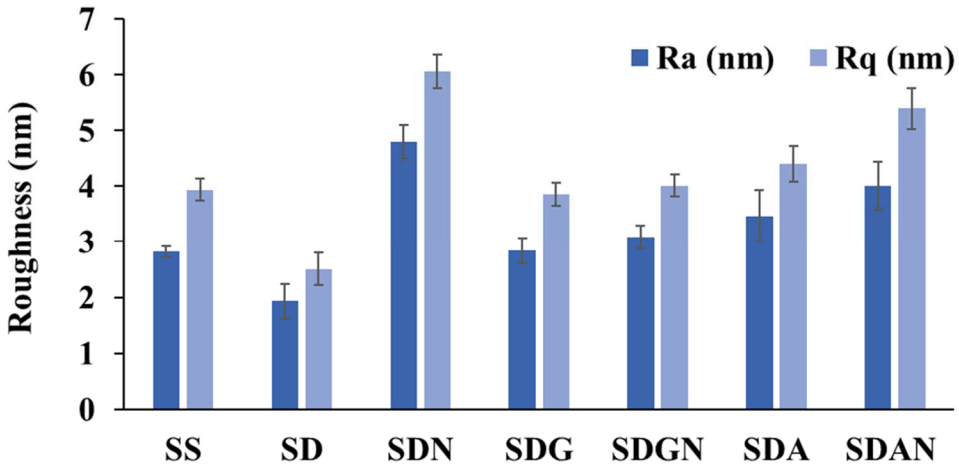

Fig. 9. Surface roughness parameters R_a and R_q for bare SS and coated SS surfaces.

On the same wave, the thickness results showed for SD a value of 310 ± 7 nm. After nisin addition to SD, the SDN thickness value increased significantly to 356 ± 10.3 nm. Otherwise, the thickness of SDG and SDA was 321.6 ± 3.7 nm and 327.6 ± 3.05 nm respectively. After nisin addition to SDG and SDA, the thickness values of SDGN and SGAN barely increased to 326.6 ± 5.03 nm and 337.6 ± 2.08 nm respectively (Fig. 10).

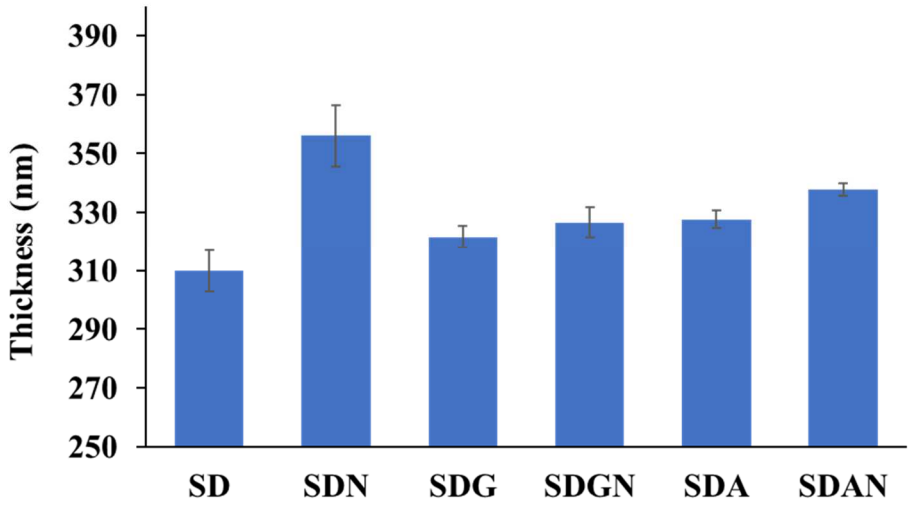

Fig. 10. Thickness of treated surfaces defined by averaged values in nm ± SD.

Aiming to visualize the morphological modifications after molecular grafting on SS, SEM analyze was carried out. Micrographs, shows that bare SS surface is smooth with small holes and crevices. Otherwise, SD is characterized by granular spherical structures that result from the 3D polymerization of dopamine. Moreover, the two-layers coatings, SDG, SDA and SDN shows a shallower topography, while the three-layers coatings SDGN and SDAN are characterized by bigger granular structures (Fig. 11).

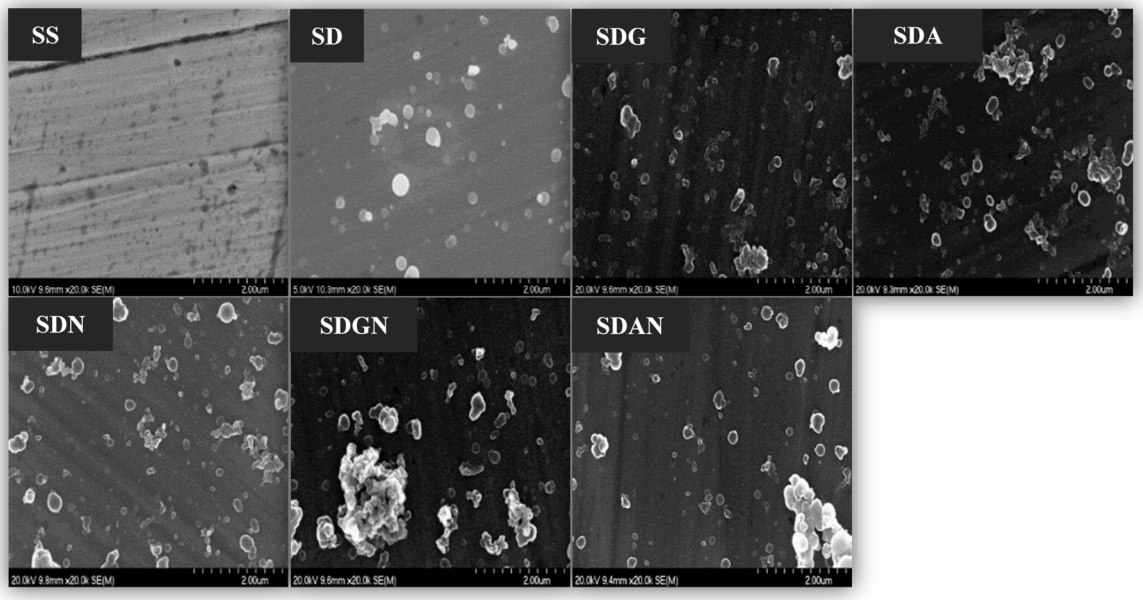

Fig. 11. Scanning electron microscopy micrographs of bare SS coated surfaces.

After SEM visualization, ion polishing was carried out in order to detect variations in the different coatings structure of SD, SDGN, SDAN and SDN, as given in Fig. 12. The cross-section showed variable specifications of each coating type. The micrographs A and B representing SD sample showed a full coverage of SS and polymerized dopamine mass respectively.

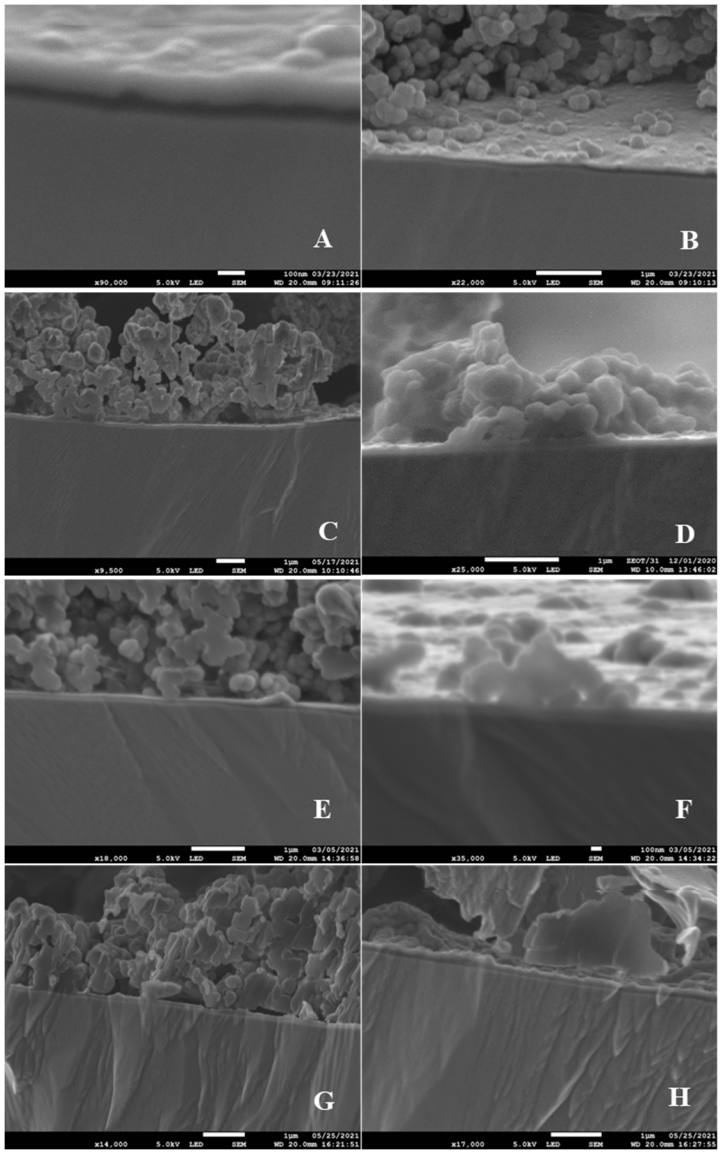

Fig. 12. SEM micrographs of cross section of coated surfaces after ion beam polishing. SD (A-B), SDGN (C-D), SDAN (E-F), SDN (G-H).

SDGN samples were represented by C and D micrographs where a mass of polydopamine/Glutaraldehyde/Nisin was detected on the sample with a full coverage preservation. E and F shows SDAN polished samples where the mass of polydopamine/Succinic acid/Nisin was detected. However, holes were detected on the sample (Micrograph F). The micrographs G and H presents the SDN coating samples. A low coverage of polydopamine and nisin accumulation was detected on G and H respectively.

ATR-FTIR analysis was performed to characterize and determine changes in the infrared bands related to the nisin immobilization on the polydopamine coated SS surfaces. Normalized FTIR spectra of nisin and grafted nisin on the polydopamine coated surface are presented in Fig. 13. Free nisin exhibited characteristic absorption bands at 3296 cm^{-1} (axial O–H and N–H stretching vibrations), 2962 cm^{-1} (C–H stretching vibrations), 1640 cm^{-1} (the absorption peak of amide band), 1514 cm^{-1} (bending of primary amines), 1441 cm^{-1} (COO symmetric stretching vibrations), and 1234 cm^{-1} (C–N stretching vibrations) [21]

FTIR spectra of different treated SS surfaces showed a broadening and shift in N–H stretching peak of nisin to higher wavenumber, which indicated that a new intermolecular H-bonding between N–H groups of nisin with O–H stretch of polydopamine in the case of SDN, succinic acid in the case of SDAN, and glutaraldehyde in the case of SDGN [22]. Amide groups of nisin most likely caused a shifting in the wavenumbers when grafted onto polydopamine coatings, without linker in the case of SDN (1600 cm^{-1}) or with linker in the case of SDAN (1607 cm^{-1}) and SDGN (1606 cm^{-1}). These subtle alterations may suggest that the intermolecular interactions exist between amino groups of the nisin and polydopamine without or with addition of linkers [23]. Besides, the nisin immobilization on the polydopamine coated SS surface caused an increase in the wavenumber of COO^- from 1244 cm^{-1} in free nisin to 1290 cm^{-1} approximatively in SDN, SDAN and SDGN. This change is probably attributed to the

existence of intermolecular interactions between nisin and polydopamine in both cases, without and with addition of linkers (succinic acid or glutaraldehyde).

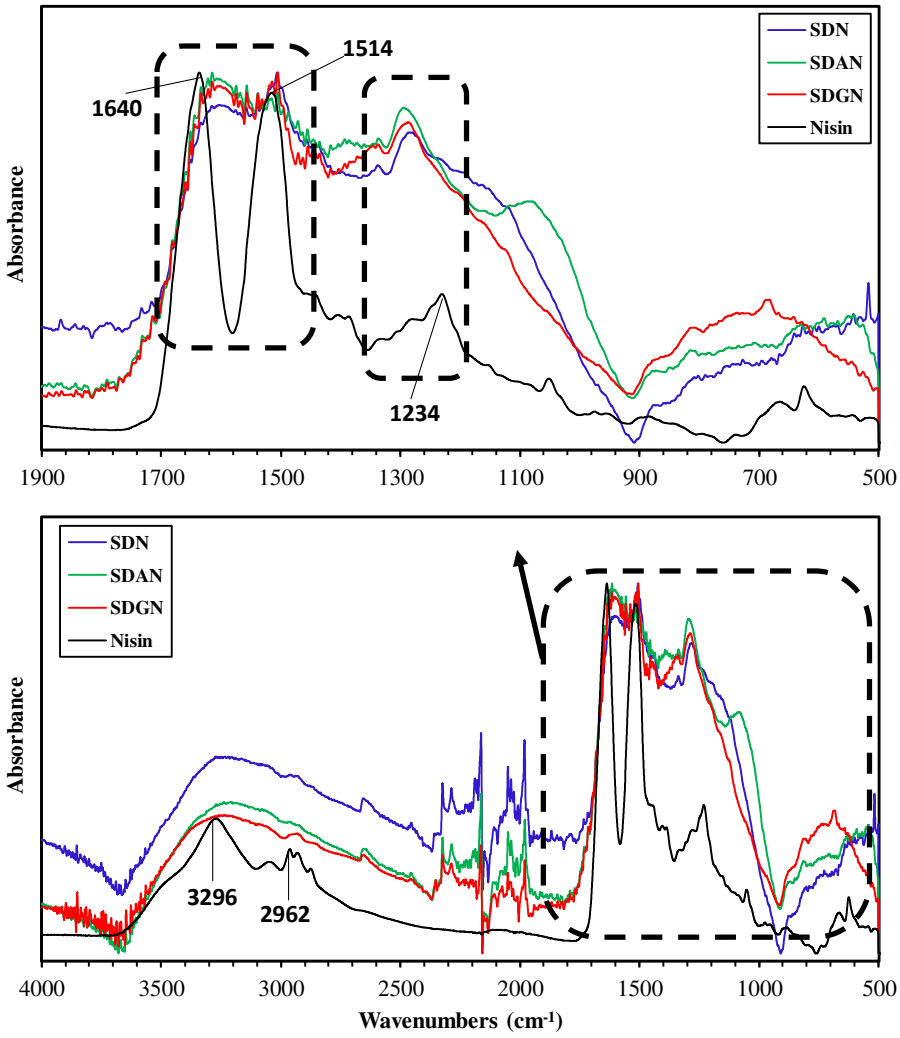

Fig. 13. FTIR spectra of different Nisin based coated SS surfaces.

ToF-SIMS spectra showed the relative intensity counts of the secondary ions corresponding to a molecular compound present on the grafted samples. Table 2 summarized the secondary ions detected by ToF-SIMS analyses of all coated surfaces SD, SDG, SDA, SDN, SDGN and SDAN and the main characterizations concerning the quantifications and the differences between surfaces. Fig. 14 represents the spectra of the three detected secondary ions

$C_8H_7NO_2^+$, $C_{12}H_{28}N^+$ and $C_{23}H_{20}N_3O_4^+$ at *m/z* 149.04, 186.24 and 402 respectively. These ions are relative of dopamine. The highest intensity was detected for SD treated surfaces, this intensity decreased with the addition of molecular layers on SD coating.

Table 2

ToF-SIMS main characterizations.

Positive and negative secondary ions	*m/z*	Related compound	Coating type with high spectra intensity count	References
$C_8H_7NO_2^+$	149.04	Dopamine hypochloride: $C_8H_{11}NO_2$	SD	[24,25]
$C_{12}H_{28}N^+$	186.24	Dopamine hypochloride: $C_8H_{11}NO_2$	SD	[26,27]
$C_{23}H_{20}N_3O_4^+$	402	Dopamine hypochloride: $C_8H_{11}NO_2$	SD	[28]
$C_3H_5O^+$	57.03	Glutaraldehyde: $C_5H_8O_2$	SDGN > SDG	[29]
$C_{12}H_{26}^+$	170.2	Succinic acid: $C_4H_6O_4$	SDA > SDAN	[30]
$C_4H_9^+$	57.06	Succinic acid: $C_4H_6O_4$	SDA > SDAN	[30]
NH_4^+	18.03	$C_8H_{11}NO_2$ and all nisin amino acids	SDGN > SDN > SDAN	[31-33]
$C_2H_5S^+$	61.01	Methionine (Met) of nisin	SDGN > SDAN > SDN	[31-33]
S_2^{2-}	31.9	^{32}S (95,02 %) of nisin	SDGN > SDAN > SDN	—
Fe^+	55.95	SS containing Fe	SDN > SDA > SDG	—

Fig. 15 represented the spectrum of the secondary ion $C_3H_5O^+$ detected at m/z 57.03. This ion corresponds to glutaraldehyde molecule. The intensity was the highest for SDG and SDGN containing glutaraldehyde. The succinic acid was detected via two secondary ions $C_4H_9^+$ and $C_{12}H_{26}^+$ spectra represented at *m/z* values are 57.06 and 170.2, respectively. The intensity count was the most important for coatings containing succinic acid SDA and SDAN. The highest intensity was for SDA then for SDAN in which the nisin covered succinic acid compound (Fig. 16). Nisin was detected by three different secondary ions. NH_4^+ spectrum was

detected at *m/z* = 18.03. This ion corresponds to dopamine containing amino groups or for nisin containing 34 amino acids. The intensity was the highest for SDGN then SDN then SDAN. Methionin amino acid of nisin was detected on the spectrum of the secondary ion $C_2H_5S^+$ at *m/z* = 61.01. Moreover, the negative secondary ion S_2^{2-} was detected at *m/z* = 31.9. For both spectra, the intensity was the highest for SDGN then SDAN then SDN (Fig. 17). In order to understand the homogeneity of the treated surfaces, the iron spectrum was analyzed. Iron secondary ion spectrum was detected on *m/z* = 55.95. The intensity counts from the highest to the lower was in the following order: SDN, SDA, SDG, SDAN, SDGN and SD (Fig. 18).

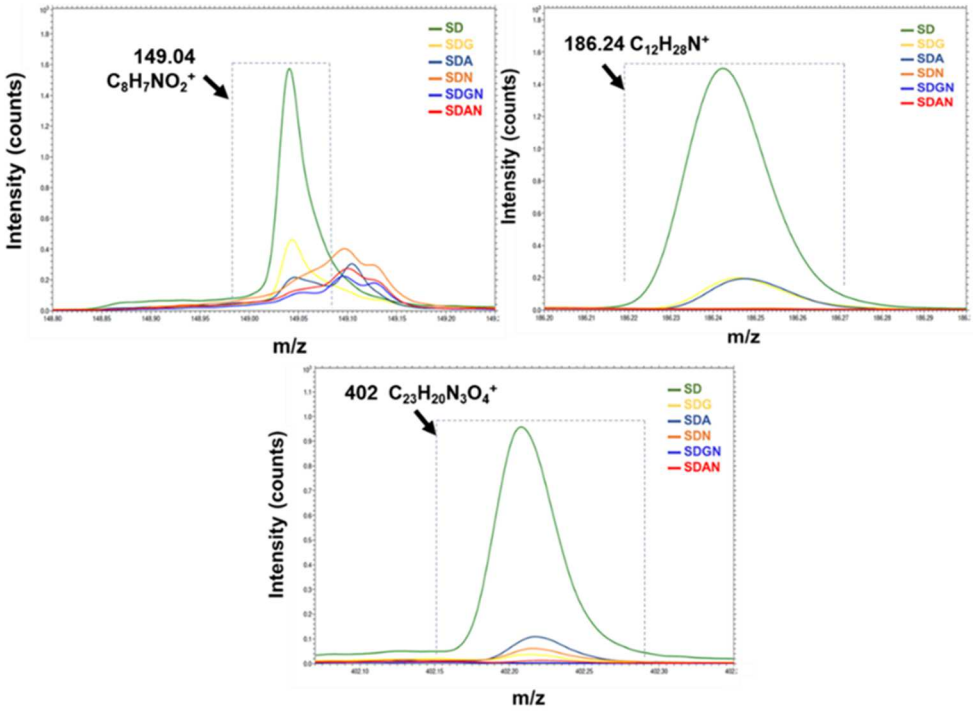

Fig. 14. ToF-SIMS spectra representing dopamine secondary ions.

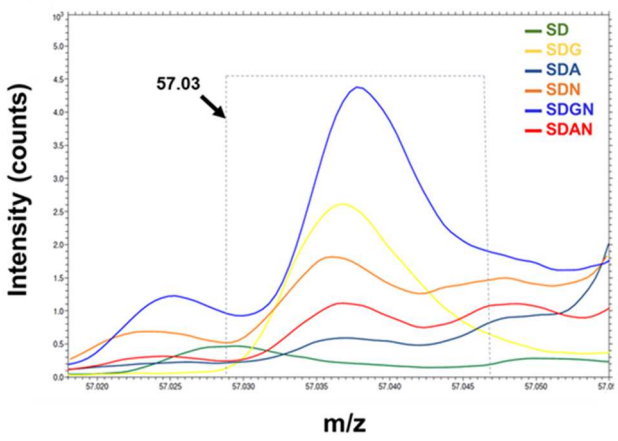

Fig. 15. ToF-SIMS spectra representing glutaraldehyde secondary ions.

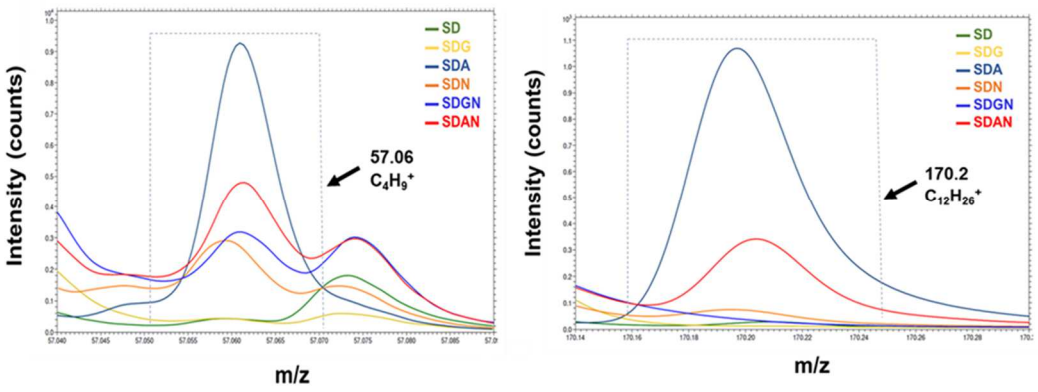

Fig. 16. ToF-SIMS spectra representing succinic acid secondary ions.

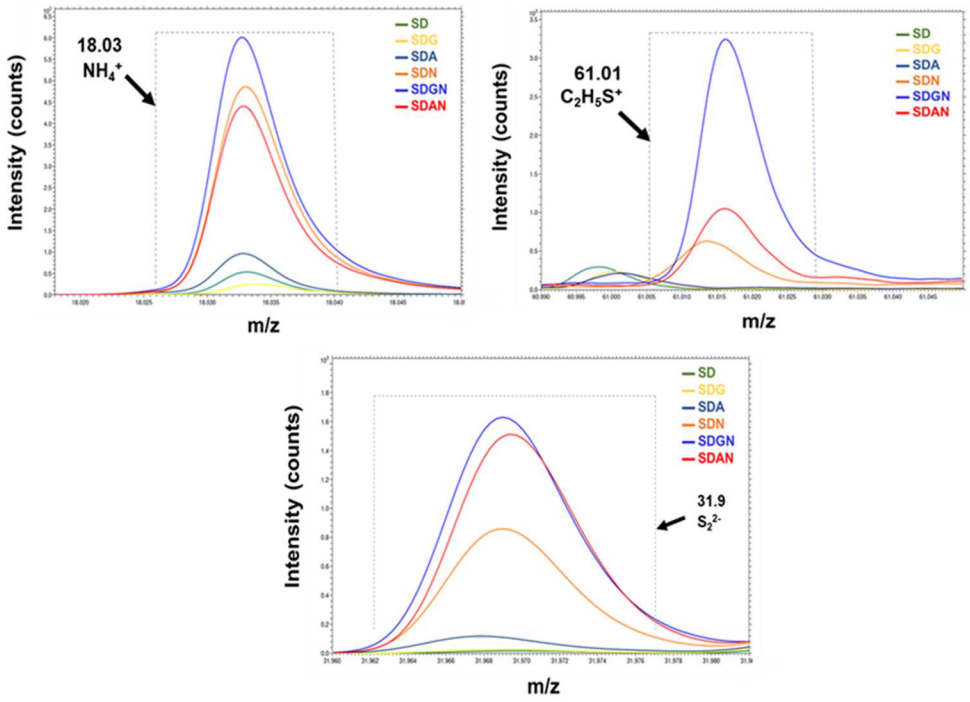

Fig. 17. ToF-SIMS spectra representing nisin secondary ions.

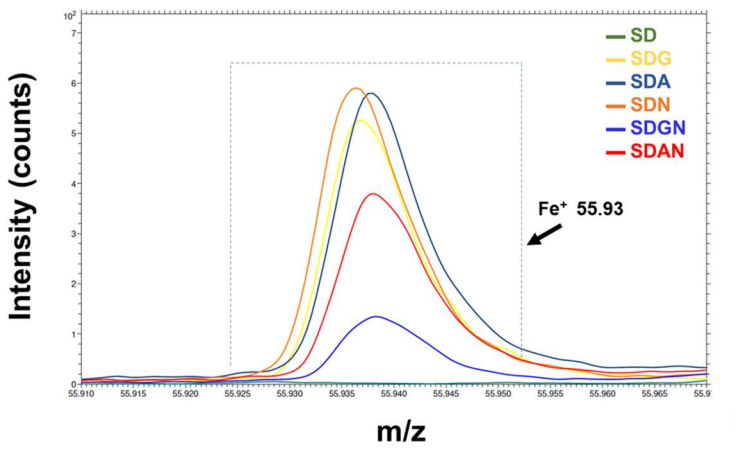

Fig. 18. ToF-SIMS spectra representing iron present in stainless steel.

XPS analyses were performed to provide the elemental composition and the distribution of functional groups of the formed layer on the different polydopamine coated SS surfaces without and with addition of nisin. The obtained XPS wide-scan (survey) spectra of different coated SS surfaces (SD, SDN, SDAN and SDGN) are shown in Fig. 19. The low intensity of the Fe2p signals in all cases is probably due to the higher coatings thickness on the SS. The obtained high-resolution peaks for C 1s, O 1s and N 1s core levels, through a deconvoluted fitting procedure using the CASA XPS software, were given in Fig. 20. The obtained values of binding energy (BE, eV), the corresponding quantification (%) as well as their assignment for each component were given in Table 3. XPS surface elemental analyses of different coated SS surfaces (SD, SDN, SDAN and SDGN) were performed and given in Table 4. In all cases, the sum of the atom concentrations was normalized to 100% in order to easily compare surface concentrations for the different elements. Carbon and oxygen atomic percentages showed no significant difference between the different coated SS surfaces. However, nitrogen atomic percentage increased significantly after nisin addition for all treated surfaces. The maximum N content value was found in the case of SDGN. Moreover, the sulfur element was absent for SD and the highest value was observed for SDGN followed by SDN and SDAN. The percentage of iron was nil on SD and SDGN while it was detected (very low) on SDN and SDAN. Hence

it is clear that glutaraldehyde linker has a significant contribution in the covalently incorporation nisin on the coating.

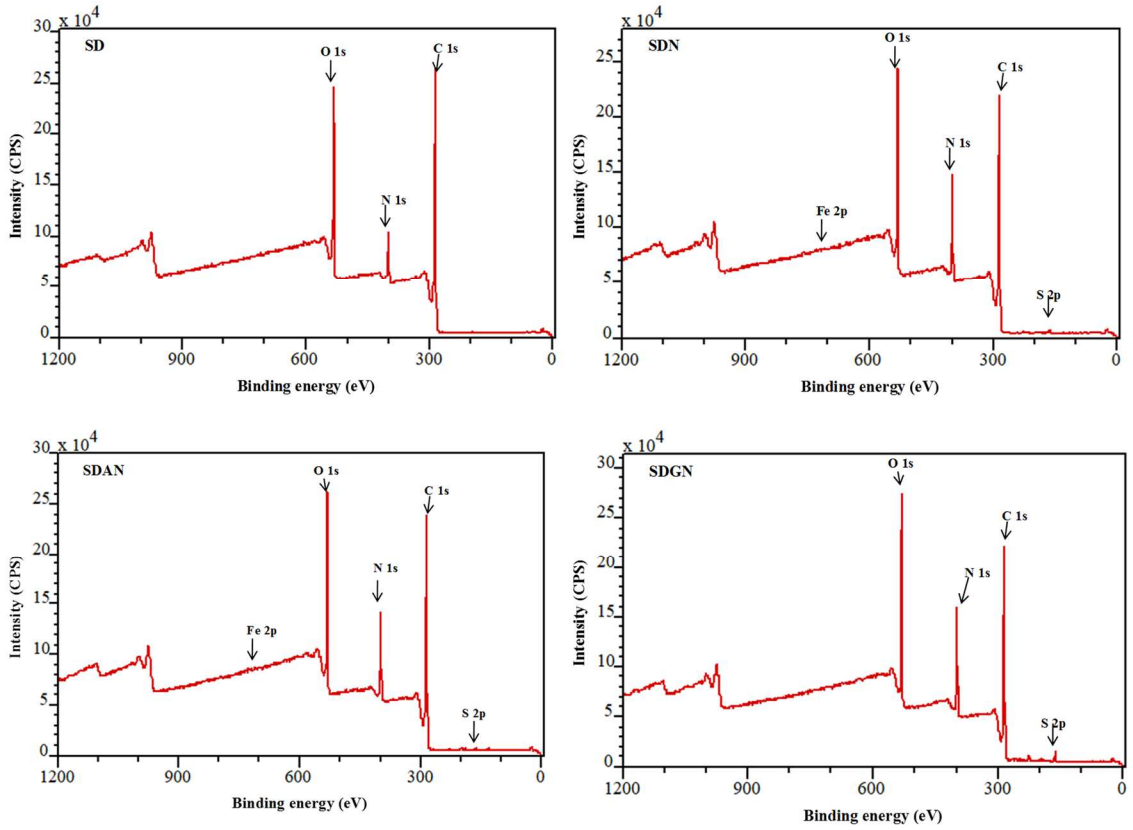

Fig. 19. XPS survey spectra of different coated SS surfaces.

The C 1s peak deconvolution for polydopamine coated SS surfaces without incorporation of nisin (SD), and with its incorporation without linker addition (SDN) and with linker addition (SDAN, SDGN) may be fitted into three components as shown in Fig. 20 and Table 3. SD shows two dominant components attributed to the C–C, C=C and C–H bonds at 284.8 eV and C–N/C–O at 286.2 eV of dopamine polymerized structure and one small component attributed to C=O at 287.8 eV that corresponds to possible tautomers of polydopamine [34]. The incorporation of nisin onto polydopamine coated SS surfaces without or with linker addition reveals a significant increase in the contribution of the component at high binding energy side, probably due to the apparition of –COOH and –CONH groups.

Indeed, all nisin characteristic functions were observed on the coatings and C 1s results permitted to confirm the nisin covalent incorporation into the different investigated coatings (SDN, SDAN, SDGN).

The O 1s region of SD, given in Fig. 20, is fitted in two peaks at 531.2 and 533.0 eV assigned to O=C and O–C species, respectively. The XPS deconvoluted O 1s spectra of SDN, SDAN and SDGN support that the incorporation of nisin without and with linker addition increase the percentage of C=O in the coatings, which prove that the nisin molecules were successfully linked into the different coated SS surfaces.

The N 1s region of SD surface is fitted into two components at 400.2 and 402.3 eV (Fig. 20). The first one represents the most contribution (91 %) and can be assigned to secondary amine (R–NH–R), while the second component can be attributed to the primary amine ($R–NH_2$) functionality [35]. Indeed, the secondary amine component dominates the N 1s region, as it is associated to polydopamine. In the case of SDN surface, the N 1s spectrum is fitted into two components, the small one (4%) at 402.2 eV attributed to the primary ($R–NH_2$) and the dominant one (96 %) assigned to the secondary (R–NH–R), and tertiary/aromatic (=N–R) amine functionalities [35]. The secondary amine is associated to both polydopamine and nisin, and the tertiary amine is associated to nisin only. The same behaviour was observed in the case of SDAN coating. However, the main component at 399.9 eV can be also attributed to the formation of amid functional group as result of the reaction of NH_2 group of nisin with the succinic acid used as linker in the SDAN coating. On the other hand, the N 1s peak was shifted to lower binding energy side for the SDGN coating, compared to other coatings (SD, SDN and SDAN) as shown in Fig. 20. The high resolution deconvoluted XPS spectra of N 1s peaks for SDGN surface show two types of nitrogen at 399.4 eV for tertiary/aromatic (=N–R) amine, 399.9 eV for the secondary (R–NH–R) amine type. It is worth noting that the primary ($R–NH_2$) amine has disappeared, and the quantification result, given in Table 3, shows that the

percentage of =N−R was the highest (88 %). This can be explained by the possible formation of imine functional group, resulting of the reaction of NH_2 group of nisin with the glutaraldehyde used as a linker in the SDGN coating.

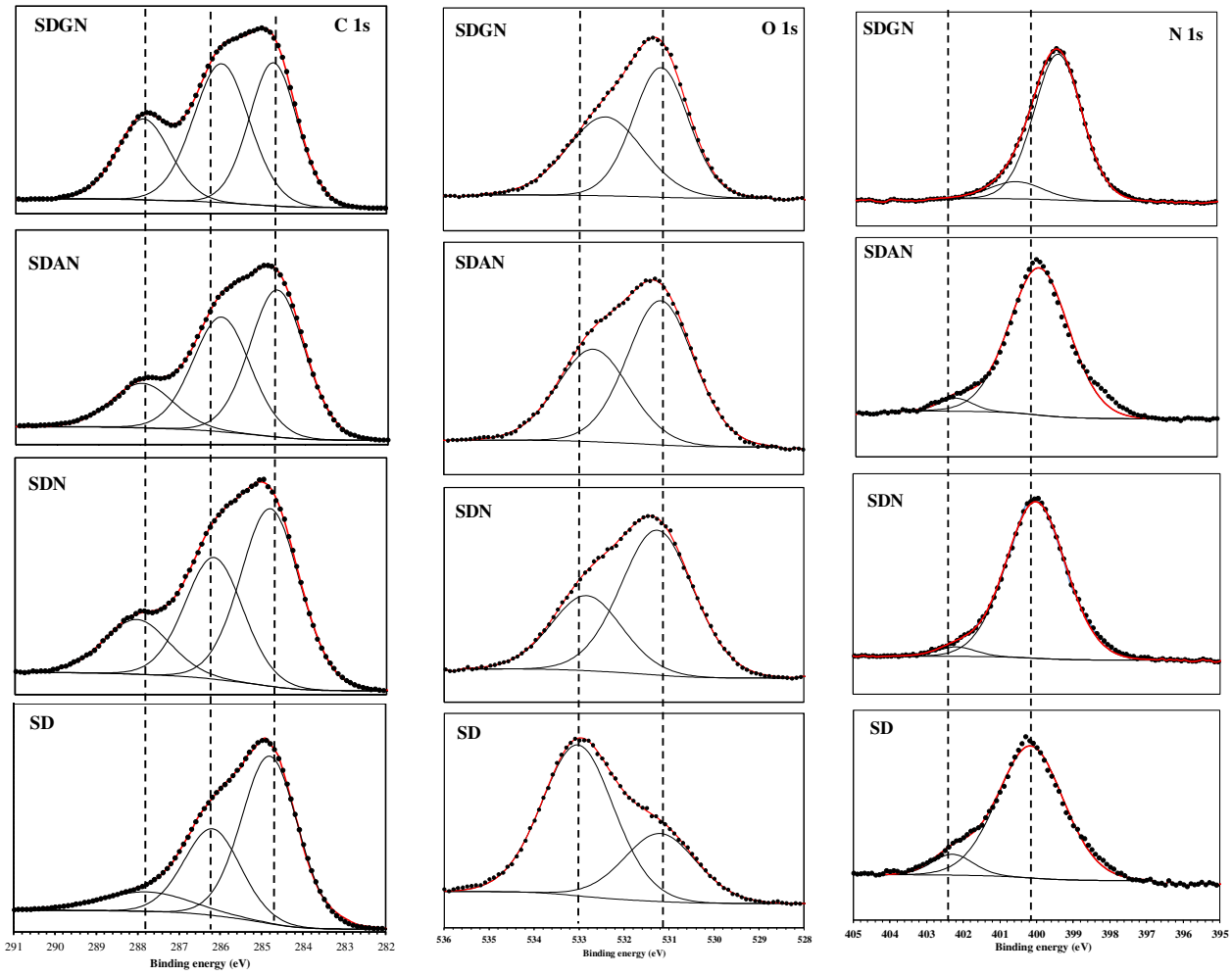

Fig. 20. High-resolution X-ray photoelectron deconvoluted profiles of C 1s, O 1s and N 1s for different coated SS surfaces.

Table 3
Binding energies (eV), relative intensity and their assignment for the major core lines observed different coated SS surfaces.

Element	Position (eV)	Assignment
	SD	
C 1s	284.8 (59 %)	C–H / C–C / C=C
	286.2 (30 %)	C–N / C–O
	287.8 (11 %)	C=O
O 1s	531.2 (32 %)	O=C
	533.0 (68 %)	O–C
N 1s	400.2 (91 %)	–NH
	402.3 (9 %)	$–NH_2$
	SDN	
C 1s	284.8 (50 %)	C–H / C–C / C=C
	286.2 (33 %)	C–O / C–N / C=N / C–S
	288.1 (17 %)	–COOH / –CONH
O 1s	531.3 (66 %)	O=C
	532.8 (34 %)	O–C
N 1s	399.9 (96 %)	=N– structure / –NH
	402.2 (4 %)	$–NH_2$
	SDAN	
C 1s	284.7 (47 %)	C–H / C–C / C=C
	286.0 (38 %)	C–O / C–N / C=N / C–S
	287.9 (15 %)	–COOH / –CONH
O 1s	531.2 (59 %)	O=C
	532.7 (41 %)	O–C
N 1s	399.9 (95 %)	=N– structure / –NH
	402.2 (5 %)	$–NH_2$
	SDGN	
C 1s	284.4 (37 %)	C–H / C–C / C=C
	285.6 (40 %)	C–O / C–N / C=N / C–S
	287.5 (23 %)	–COOH / –CONH
O 1s	530.8 (51 %)	O=C
	532.0 (49 %)	O–C
N 1s	399.4 (88 %)	=N– structure
	400.6 (12 %)	–NH

Table 4

Atomic percentage of atoms (%) on coated SS surfaces by XPS.

Atom	SD	SDN	SDGN	SDAN
C	76.62	70.14	67.87	70.38
O	16.17	16.60	16.66	17.35
N	7.16	12.83	14.40	11.91
S	0.00	0.34	1.07	0.20
Fe	0.00	0.10	0.00	0.16

4. Discussion

The antimicrobial grafting on materials used in medical and food sectors, like SS, constitutes a promising way forward. In this research, bacteriocin nisin produced by *Lactococcus lactis* subsp *lactis*, was successfully grafted on the surface of SS. The aim of this study was to investigate the antimicrobial effect and chemical properties of elaborated coatings. After ensuring that the bacterial adhesion rate was similar and comparable on all coated surfaces, the antimicrobial tests were carried out. Nisin was grafted onto the steel according to two approaches using its $–NH_2$ and –COOH groups (Fig. 2). Moreover, studies on nisin mechanism suggested that its effective action requires the presence of its carboxylic and amino groups in a non-linked state [10,36,37]. However, the challenge test results showed an effective antimicrobial activity for SDGN followed by SDAN when nisin is linked by its amino group keeping the carboxylic terminal group free. The antimicrobial effect was the most efficient after 3 and 5 h of contact while the bacterial population increased after 24 h. These results suggest single use surfaces of these coatings. Otherwise, for SDN samples, nisin's carboxylic group was linked and its amino group was free, the challenge test did not reveal an antimicrobial effect. This demonstrates the implication of hydrophilic side of nisin, containing the non-linked –COOH, in the antimicrobial activity. On the same wave, the viability percentages of *L. monocytogenes* decreased of almost 70 % for SDGN and SDAN while no decrease was detected for SDN.

The antibacterial qualitative assessment demonstrated bacterial efficiency only for SDGN and SDAN and that nisin linkage to these coatings inhibited its diffusion while free nisin soaked in a cellulose disc showed an inhibition zone due to its diffusion. Nisin mode of action was highlighted by the MEB analysis of the effective antibacterial SDGN and SDAN. Indeed, the micrographs presented the damaged bacterial membrane of dead *L. monocytogenes*. In order

to understand these difference of antimicrobial efficacy between SDGN, SDAN and SDN, surfaces properties were characterized chemically and morphologically.

WCA is a technique that is sensitive to the extreme surface of a coating [38]. It was carried out for all elaborated surfaces in order to detect hydrophobicity modification after molecules grafting. Indeed, the hydrophobicity increased on SDN, SDAN and SDGN proving nisin attachment to samples. Furthermore, studies have shown that the hydrophilicity of a surface may contribute in the prevention of bacterial contamination of coated surfaces [39,40]. However, the antibacterial tests showed that nisin-coated surfaces were not all antimicrobial while WCA measurements were of the same order. Indeed, the hydrophilic character of nisin-coated surfaces was not involved in the antimicrobial efficiency.

FTIR analyses permitted the detection of functional groups linked to nisin molecule in the free and grafted state. The results gave the evidence that nisin was attached to the polydopamine coating. In all coated surfaces SDN, SDGN and SDAN, intramolecular interactions between polydopamine and nisin were detected regardless the presence of linkers or not between the two molecules.

ToF-SIMS and XPS analyses were carried out to understand nisin conformation and quantitative aspects of elements on the coatings. Tof-SIMS spectra showed the relative intensity counts of the secondary ions corresponding to each grafted compound present on the samples. The depth profiling limit of Tof-SIMS was around few nanometers. Each compound grafted in the external layer of each developed coating was identified via the secondary ions and analyzed quantitatively and qualitatively. Polydopamine, glutaraldehyde and succinic acid were identified on the coatings already containing each compound. For dopamine, when layers were added, the intensity count of the ion corresponding to the internal layer decreased (SD > SDG-SDA-SDN > SDGN-SDAN). Concerning nisin specific secondary ions, the intensity counts of each ion was compared between SDN, SDAN and SDN containing nisin. NH_4^+ spectra showed

the highest intensity for SDGN then for SDN then for SDAN. Otherwise, $C_2H_5S^+$ and S_2^{2-} spectra intensity followed the level of antibacterial efficiency, from efficient to less efficient to inefficient. Indeed, the intensity for both ions was the highest for SDGN then SDAN then SDN. The intensity of NH_4^+ spectra was higher for SDN than SDAN due to the presence of polydopamine directly linked to nisin in SDN. Indeed, NH_4^+ is a secondary ion representing dopamine and nisin at the same time. The SDN peak intensity of NH_4^+ represented both nisin and polydopamine. Therefore, nisin quantity was the highest for SDGN then SDN then SDAN. Moreover, $C_2H_5S^+$ secondary ion representing the methionine amino acid located at sites 17 and 21 of nisin that are closer to the side containing the carboxylic terminal group. This ion was more pronounced for SDGN and SDAN where nisin –COOH side is free than for SDN where nisin –COOH side is engaged. This result permitted to confirm the nisin orientation. Moreover, in order to investigate the coatings homogeneity, Fe^+ intensity peaks showed that SD was fully covered by polydopamine and the coating was homogeneous. For SDN, SDG and SDA, the nisin, glutaraldehyde and succinic acid addition on SD respectively, guided the polydopamine with it and SS bare surface was detected via Fe^+ ions. However, For SDGN and SDAN, the nisin addition on SDG and SDA decreased the intensity peak of $Fe^{+\cdot}$ The decrease was more important for SDGN than SDAN. Indeed, SDGN was considered homogeneous while SDAN presented some heterogeneities.

XPS results were in concordance with ToF-SIMS. The sampling depth of XPS analysis is approximatively of 70 nm. The atomic percentage of nitrogen was the most important for SDGN followed by SDN then SDAN. The nitrogen percentage of SDN was higher than SDAN because of the presence of nitrogen in polydopamine, detected for SDN. The percentage of sulfur was nil on SD due to the absence of nisin containing disulfide bridges. SDGN had the highest atomic percentage followed by SDN and SDAN. The atomic percentage of iron, on the same wave of ToF-SIMS results, was nil for SD and SDGN and detected for SDN and SDAN.

The XPS survey spectra certified the interpretation of ToF-SIMS and XPS atomic percentages. Indeed, the peak analyses confirmed that nisin quantity on SDGN was the highest followed by SDN then SDAN. Moreover, the detection on iron peaks on SDN and SDAN confirmed the heterogeneity of these two coatings while SD and SDGN were homogenous and SS was fully covered. For the C 1s signal, C=N, C–S and C=O assignments detected on SDN, SDAN and SDGN represented nisin adsorption especially the carbon-sulfur bond conferring to disulphide bonds in nisin. Peaks representing the functional groups –COOH and –CONH were also detected on those three coatings with different percentages. Indeed, for SDGN, it was the highest (23%) then SDN (17%) then SDAN (15%). This percentages distribution indicated the difference in nisin quantity grafted on each surface. For the O 1s signal, on SD, H_2O adsorption was linked to its hydrophilic character while –O=C bond appeared for nisin grafted coatings. The highest percentages were detected for SDGN (49 %) and SDAN (41 %) while it was less pronounced for SDN (34 %). This difference is linked to the conformation of nisin on those surfaces. The acidic function is free and more exposed for SDGN and SDAN while nisin is linked by its carboxylic function to polydopamine on SDN (Fig. 20, Table 3).

Several studies demonstrated that the increase in a surface roughness induces a decrease in the antimicrobial effect [41-44]. Moreover, a rough surface provides an adequate environment for the bacteria to adhere on a surface and generates a biofilm. These results are consistent with the literature, SDN coating was inactive against *L. monocytogenes* while its surface roughness was the highest. However, SDGN and SDAN registered the lowest surface roughness and showed an effective antimicrobial activity. Indeed, the use of several approaches in grafting nisin may lead to its conformation modification on the surface that can be the cause of the variation of surface roughness and antimicrobial activity.

Roughness and thickness results illustrated the morphology of each coating type. Roughness and thickness of SDN after nisin addition increased significantly while it barely

increased after nisin addition to SDA and SDG. Indeed, nisin tended to accumulate on SDN while it is distributed evenly without increasing the roughness and thickness of SDGN and SDAN. Moreover, the presence of iron detected on SDAN and SDN proved their heterogeneity. Nisin accumulation and iron presence on SDN demonstrate a columnar coating. This accumulation and chemical bonding might be the cause of nisin inactivity towards *L. monocytogenes*. Otherwise, SDGN and SDAN seems to present a similar structure despite the presence of coverage heterogeneity on SDAN (Fe detection). The antimicrobial highest effectiveness of SDGN was linked to nisin highest quantity adsorption, to nisin free carboxylic group playing a role in antibacterial mechanism and to homogeneity of the coating. Moreover, SDAN antimicrobial effectiveness was linked to nisin chemical linkage with a free carboxylic group like SDGN and nisin distribution on succinic acid without its accumulation. The diminution of its activity in comparison with SDGN is linked to nisin lower quantity and heterogeneity in the coverage. SEM of coatings permitted to show the global morphology and detect different morphologies after molecules grafting. It showed the surface from the top but did not allow to see some other differences in coating microstructure such as columnar aspect, porosity and stainless steel/dopamine interface, …. Therefore, ion polishing was carried out to analyse the cross section of each coating. The observed microstructural variations of the different coatings were in concordance with FTIR, XPS, ToF SIMS, roughness and thickness analysis. Indeed, SD was homogeneous and polymerized dopamine was detected and the surface was fully covered. Moreover, SDGN was also homogeneous and the surface was fully covered. The presence of porosity in SDAN micrographs outlined the Fe detection by ToF SIMS. This explains why the antimicrobial effectiveness of SDGN was higher than SDAN. Otherwise, SDN micrographs showed a non-homogenous and non uniform covering coating presenting nisin accumulation in a tubular aspect. The accumulation and chemical conformation of nisin initially linked via its carboxylic group lead to the inactivation of antimicrobial efficacy.

Moreover, these results explain the high roughness and thickness of SDN after nisin addition in comparison with SDGN and SDAN.

Conclusions

This study permitted to reach the main goal concerning the prevention of biofilm formation on SS surface in order to protect population health. The functionalized surfaces were analyzed chemically and biologically. Challenge tests, antibacterial qualitative testing, SEM and LIVE/DEAD techniques towards *L. monocytogenes* demonstrated the antimicrobial effectiveness of SDGN followed by SDAN and the non-efficient activity of SDN. The chemical grafting of molecules on the different prepared surfaces provided information of nisin linkage conformation on each surface. The results showed that nisin was linked in SDGN and SDAN by its amino group to glutaraldehyde and succinic acid respectively, and in SDN by its carboxylic group to polydopamine. Moreover, ToF-SIMS, XPS, surface roughness and thickness analysis, ionic polishing and WCA enabled the understanding of surfaces homogeneities, nisin presence and quantification, and coatings qualifications. Indeed, those analyses showed that the nisin carboxylic group participate in the antibacterial effect.

Acknowledgement

The authors thank MOBLILEX program of the Université de Lille for their financial support.

References

[1] M. Abdallah, C. Benoliel, D. Drider, P. Dhulster, N.-E. Chihib, Biofilm formation and persistence on abiotic surfaces in the context of food and medical environments, Arch. Microbiol. 196 (2014) 453–472. https://doi.org/10.1007/s00203-014-0983-1.

[2] H. Wu, C. Moser, H.-Z. Wang, N. Høiby, Z.-J. Song, Strategies for combating bacterial biofilm infections, Int. J. Oral Sci. 7 (2015) 1–7. https://doi.org/10.1038/ijos.2014.65.

[3] World Health Organization, ed., WHO estimates of the global burden of foodborne diseases, World Health Organization, Geneva, Switzerland, 2015.

[4] Bates DW, Larizgoitia I, Prasopa-Plaizier N, Jha AK., Global priorities for patient safety research. BMJ 2009; 338: b1775., (2009). https://www.ncbi.nlm.nih.gov/pubmed/19443552 (accessed October 3, 2019).

[5] J.P. Burke, Infection Control — A Problem for Patient Safety, N. Engl. J. Med. 348 (2003) 651–656. https://doi.org/10.1056/NEJMhpr020557.

[6] Pittet D., Donaldson L., Clean Care is Safer Care: a worldwide priority. - PubMed - NCBI, (2005). https://www.ncbi.nlm.nih.gov/pubmed/16214584 (accessed October 3, 2019).

[7] L. Karam, C. Jama, N. Nuns, A.-S. Mamede, P. Dhulster, N.-E. Chihib, Nisin adsorption on hydrophilic and hydrophobic surfaces: evidence of its interactions and antibacterial activity: NISIN INTERACTIONS AND ACTIVITY ON HYDROPHILIC OR HYDROPHOBIC SURFACES, J. Pept. Sci. 19 (2013) 377–385. https://doi.org/10.1002/psc.2512.

[8] Albanese Donatella, Garofalo Francesca, Pilloton Roberto, Capo Salvatore, Malvano Francesca, Development of an Antimicrobial Peptide-based Biosensor for the Monitoring of Bacterial Contaminations, Chem. Eng. Trans. 75 (2019) 61–66. https://doi.org/10.3303/CET1975011.

[9] S. Chandrapati, D.J. O'Sullivan, Procedure for quantifiable assessment of nutritional parameters influencing nisin production by Lactococcus lactis subsp. lactis, J. Biotechnol. 63 (1998) 229–233. https://doi.org/10.1016/s0168-1656(98)00090-x.

[10] I.A. Kassaa, R. Rafei, M. Moukhtar, M. Zaylaa, A. Gharsallaoui, A. Asehraou, K.E. Omari, A. Shahin, M. Hamze, N.-E. Chihib, LABiocin database: A new database designed specifically for Lactic Acid Bacteria bacteriocins, Int. J. Antimicrob. Agents. 54 (2019) 771–779. https://doi.org/10.1016/j.ijantimicag.2019.07.012.

[11] M. Vukomanović, V. Žunič, Š. Kunej, B. Jančar, S. Jeverica, R. Podlipec, D. Suvorov, Nano-engineering the Antimicrobial Spectrum of Lantibiotics: Activity of Nisin against Gram Negative Bacteria, Sci. Rep. 7 (2017) 4324. https://doi.org/10.1038/s41598-017-04670-0.

[12] H.Y. Cui, J. Wu, C.Z. Li, L. Lin, Anti-listeria effects of chitosan-coated nisin-silica liposome on Cheddar cheese, J. Dairy Sci. 99 (2016) 8598–8606. https://doi.org/10.3168/jds.2016-11658.

[13] X. Chen, X. Zhang, R. Meng, Z. Zhao, Z. Liu, X. Zhao, C. Shi, N. Guo, Efficacy of a combination of nisin and p-Anisaldehyde against Listeria monocytogenes, Food Control. 66 (2016) 100–106. https://doi.org/10.1016/j.foodcont.2016.01.025.

[14] T. Lou, X. Bai, X. He, C. Yuan, Antifouling performance analysis of peptide-modified glass microstructural surfaces, Appl. Surf. Sci. 541 (2021) 148384. https://doi.org/10.1016/j.apsusc.2020.148384.

[15] R. Schoevaart, T. Kieboom, Galactose dialdehyde as potential protein cross-linker: proof of principle, Carbohydr. Res. 337 (2002) 899–904. https://doi.org/10.1016/S0008-6215(02)00051-4.

[16] J.G. Zeikus, M.K. Jain, P. Elankovan, Biotechnology of succinic acid production and markets for derived industrial products, Appl. Microbiol. Biotechnol. 51 (1999) 545–552. https://doi.org/10.1007/s002530051431.

[17] SCOGS (Select Committee on GRAS Substances), (n.d.). https://www.cfsanappsexternal.fda.gov/scripts/fdcc/index.cfm?set=SCOGS (accessed June 28, 2021).

[18] M. Abdallah, O. Khelissa, A. Ibrahim, C. Benoliel, L. Heliot, P. Dhulster, N.-E. Chihib, Impact of growth temperature and surface type on the resistance of Pseudomonas aeruginosa and Staphylococcus aureus biofilms to disinfectants, Int. J. Food Microbiol. 214 (2015) 38–47. https://doi.org/10.1016/j.ijfoodmicro.2015.07.022.

[19] ISO 22196:2011, ISO. (n.d.). https://www.iso.org/cms/render/live/en/sites/isoorg/contents/data/standard/05/44/54431.html (accessed June 29, 2021).
[20] D.A. Shirley, High-Resolution X-Ray Photoemission Spectrum of the Valence Bands of Gold, Phys. Rev. B. 5 (1972) 4709–4714. https://doi.org/10.1103/PhysRevB.5.4709.
[21] T. Krivorotova, A. Cirkovas, S. Maciulyte, R. Staneviciene, S. Budriene, E. Serviene, J. Sereikaite, Nisin-loaded pectin nanoparticles for food preservation, Food Hydrocoll. 54 (2016) 49–56. https://doi.org/10.1016/j.foodhyd.2015.09.015.
[22] F. Gong, J. Qian, Y. Chen, S. Yao, J. Tong, H. Guo, Preparation and properties of gum arabic cross-link binding nisin microparticles, Carbohydr. Polym. 197 (2018) 608–613. https://doi.org/10.1016/j.carbpol.2018.05.080.
[23] N.A. Lopes, C.M.B. Pinilla, A. Brandelli, Pectin and polygalacturonic acid-coated liposomes as novel delivery system for nisin: Preparation, characterization and release behavior, Food Hydrocoll. 70 (2017) 1–7. https://doi.org/10.1016/j.foodhyd.2017.03.016.
[24] Y. Ding, L.-T. Weng, M. Yang, Z. Yang, X. Lu, N. Huang, Y. Leng, Insights into the Aggregation/Deposition and Structure of a Polydopamine Film, Langmuir. 30 (2014) 12258–12269. https://doi.org/10.1021/la5026608.
[25] L. Han, L. Yan, K. Wang, L. Fang, H. Zhang, Y. Tang, D. Yonghui, L.T. Weng, J. Xu, J. Weng, Y. Liu, F. Ren, X. Lu, Tough, self-healable and tissue-adhesive hydrogel with tunable multifunctionality, NPG Asia Mater. 9 (2017) e372. https://doi.org/10.1038/am.2017.33.
[26] S. Equey, Investigation of the interaction between diamond-like carbon coatings and lubricant additives, Doctoral Thesis, ETH Zurich, 2008. https://doi.org/10.3929/ethz-a-005730458.
[27] J.P. Hofmann, M. Rohnke, B.M. Weckhuysen, Recent advances in secondary ion mass spectrometry of solid acid catalysts: large zeolite crystals under bombardment, Phys Chem Chem Phys. 16 (2014) 5465–5474. https://doi.org/10.1039/C3CP54337D.
[28] Q. Lyu, N. Hsueh, C.L.L. Chai, Unravelling the polydopamine mystery: is the end in sight?, Polym. Chem. 10 (2019) 5771–5777. https://doi.org/10.1039/C9PY01372E.
[29] IONICON Analytik, (n.d.). https://www.ionicon.com/ (accessed February 15, 2021).
[30] GLOVOCS, (n.d.). http://glovocs.creaf.cat/ (accessed February 15, 2021).
[31] M. Henry, C. Dupont-Gillain, P. Bertrand, Conformation Change of Albumin Adsorbed on Polycarbonate Membranes as Revealed by ToF-SIMS, Langmuir. 19 (2003) 6271–6276. https://doi.org/10.1021/la034081z.
[32] K.F. Schilke, J. McGuire, Detection of nisin and fibrinogen adsorption on poly(ethylene oxide) coated polyurethane surfaces by time-of-flight secondary ion mass spectrometry (ToF-SIMS), J. Colloid Interface Sci. 358 (2011) 14–24. https://doi.org/10.1016/j.jcis.2011.03.014.
[33] S. Muramoto, D.J. Graham, M.S. Wagner, T.G. Lee, D.W. Moon, D.G. Castner, ToF-SIMS Analysis of Adsorbed Proteins: Principal Component Analysis of the Primary Ion Species Effect on the Protein Fragmentation Patterns, J. Phys. Chem. C. 115 (2011) 24247–24255. https://doi.org/10.1021/jp208035x.
[34] R.A. Zangmeister, T.A. Morris, M.J. Tarlov, Characterization of polydopamine thin films deposited at short times by autoxidation of dopamine, Langmuir ACS J. Surf. Colloids. 29 (2013) 8619–8628. https://doi.org/10.1021/la400587j.
[35] F. Bernsmann, A. Ponche, C. Ringwald, J. Hemmerlé, J. Raya, B. Bechinger, J.-C. Voegel, P. Schaaf, V. Ball, Characterization of Dopamine−Melanin Growth on Silicon Oxide, J. Phys. Chem. C. 113 (2009) 8234–8242. https://doi.org/10.1021/jp901188h.
[36] J. Aveyard, J.W. Bradley, K. McKay, F. McBride, D. Donaghy, R. Raval, R.A. D'Sa, Linker-free covalent immobilization of nisin using atmospheric pressure plasma induced grafting, J. Mater. Chem. B. 5 (2017) 2500–2510. https://doi.org/10.1039/C7TB00113D.
[37] D. Duday, C. Vreuls, M. Moreno, G. Frache, N.D. Boscher, G. Zocchi, C. Archambeau, C. Van De Weerdt, J. Martial, P. Choquet, Atmospheric pressure plasma modified surfaces for immobilization of antimicrobial nisin peptides, Surf. Coat. Technol. 218 (2013) 152–161. https://doi.org/10.1016/j.surfcoat.2012.12.045.

[38] N. Nagy, Contact Angle Determination on Hydrophilic and Superhydrophilic Surfaces by Using r–θ-Type Capillary Bridges, Langmuir. 35 (2019) 5202–5212. https://doi.org/10.1021/acs.langmuir.9b00442.
[39] J. Lee, H.-R. Chae, Y.J. Won, K. Lee, C.-H. Lee, H.H. Lee, I.-C. Kim, J. Lee, Graphene oxide nanoplatelets composite membrane with hydrophilic and antifouling properties for wastewater treatment, J. Membr. Sci. 448 (2013) 223–230. https://doi.org/10.1016/j.memsci.2013.08.017.
[40] H. Yu, Y. Xie, M. Hu, J. Wang, S. Wang, Z. Xu, Surface modification of polypropylene microporous membrane to improve its antifouling property in MBR: CO plasma treatment, J. Membr. Sci. 254 (2005) 219–227. https://doi.org/10.1016/j.memsci.2005.01.010.
[41] S.-J. Ahn, S.-J. Lee, J.-K. Kook, B.-S. Lim, Experimental antimicrobial orthodontic adhesives using nanofillers and silver nanoparticles, Dent. Mater. 25 (2009) 206–213. https://doi.org/10.1016/j.dental.2008.06.002.
[42] H.-W. Chen, K.-C. Hsu, Y.-C. Chan, J.-G. Duh, J.-W. Lee, J.S.-C. Jang, G.-J. Chen, Antimicrobial properties of Zr–Cu–Al–Ag thin film metallic glass, Thin Solid Films. 561 (2014) 98–101. https://doi.org/10.1016/j.tsf.2013.08.028.
[43] A. da Silva, O. Teschke, Effects of the antimicrobial peptide PGLa on live Escherichia coli, Biochim. Biophys. Acta BBA - Mol. Cell Res. 1643 (2003) 95–103. https://doi.org/10.1016/j.bbamcr.2003.10.001.
[44] R. Mauchauffé, M. Moreno-Couranjou, N.D. Boscher, C. Van De Weerdt, A.-S. Duwez, P. Choquet, Robust bio-inspired antibacterial surfaces based on the covalent binding of peptides on functional atmospheric plasma thin films, J. Mater. Chem. B. 2 (2014) 5168. https://doi.org/10.1039/C4TB00503A.

Nisin-based coatings for the prevention of biofilm formation: Surface characterization and antimicrobial assessments

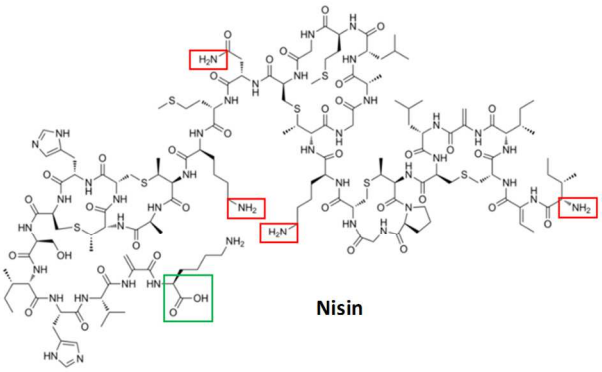

Nisin

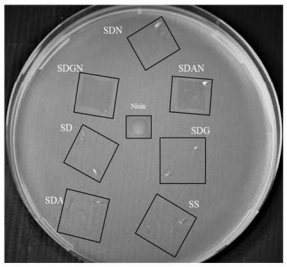

Antibacterial assessment toward *Listeria monocytogenes* of different coated SS surfaces and nisin

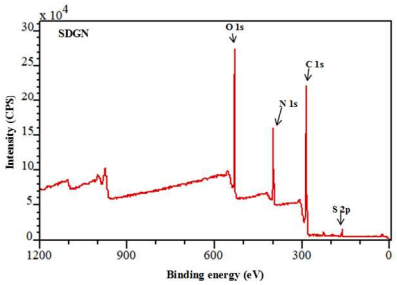

XPS analysis

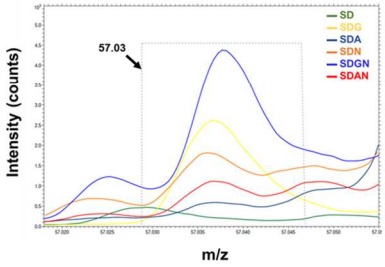

ToF-SIMS analysis